Redox Biology 24 (2019) 101192

Contents lists available at ScienceDirect

Redox Biology

journal homepage: www.elsevier.com/locate/redox

Nicotinamide mononucleotide (NMN) supplementation rescues cerebromicrovascular endothelial function and neurovascular coupling responses and improves cognitive function in aged mice

Stefano Tarantini[a], Marta Noa Valcarcel-Ares[a], Peter Toth[a,b], Andriy Yabluchanskiy[a], Zsuzsanna Tucsek[a], Tamas Kiss[a], Peter Hertelendy[a], Michael Kinter[a,c], Praveen Ballabh[d], Zoltán Süle[e], Eszter Farkas[f], Joseph A. Baur[g], David A. Sinclair[h], Anna Csiszar[a,f], Zoltan Ungvari[a,f,i,j,*]

[a] Vascular Cognitive Impairment and Neurodegeneration Program, Reynolds Oklahoma Center on Aging/Department of Geriatric Medicine, University of Oklahoma Health Sciences Center, Oklahoma City, OK, USA
[b] Department of Neurosurgery, Medical School, University of Pecs, Hungary
[c] Aging and Metabolism Research Program, Oklahoma Medical Research Foundation, Oklahoma City, OK, 73104, USA
[d] Division of Neonatology, Department of Pediatrics, Albert Einstein College of Medicine, USA
[e] Department of Anatomy, University of Szeged, Szeged, Hungary
[f] Department of Medical Physics and Informatics, University of Szeged, Szeged, Hungary
[g] Department of Physiology and Institute for Diabetes, Obesity, and Metabolism, Perelman School of Medicine, University of Pennsylvania, Philadelphia, PA 19104, USA
[h] Department of Genetics, Harvard Medical School, Boston, USA
[i] Department of Public Health, Semmelweis University, Budapest, Hungary
[j] Department of Health Promotion Sciences, College of Public Health, University of Oklahoma Health Sciences Center, Oklahoma City, OK, USA

ARTICLE INFO

Keywords:
Oxidative stress
ROS
Endothelial dysfunction
Functional hyperemia
Microcirculation

ABSTRACT

Adjustment of cerebral blood flow (CBF) to neuronal activity via neurovascular coupling (NVC) has an essential role in maintenance of healthy cognitive function. In aging increased oxidative stress and cerebromicrovascular endothelial dysfunction impair NVC, contributing to cognitive decline. There is increasing evidence showing that a decrease in NAD^+ availability with age plays a critical role in a range of age-related cellular impairments but its role in impaired NVC responses remains unexplored. The present study was designed to test the hypothesis that restoring NAD^+ concentration may exert beneficial effects on NVC responses in aging. To test this hypothesis 24-month-old C57BL/6 mice were treated with nicotinamide mononucleotide (NMN), a key NAD^+ intermediate, for 2 weeks. NVC was assessed by measuring CBF responses (laser Doppler flowmetry) evoked by contralateral whisker stimulation. We found that NVC responses were significantly impaired in aged mice. NMN supplementation rescued NVC responses by increasing endothelial NO-mediated vasodilation, which was associated with significantly improved spatial working memory and gait coordination. These findings are paralleled by the sirtuin-dependent protective effects of NMN on mitochondrial production of reactive oxygen species and mitochondrial bioenergetics in cultured cerebromicrovascular endothelial cells derived from aged animals. Thus, a decrease in NAD^+ availability contributes to age-related cerebromicrovascular dysfunction, exacerbating cognitive decline. The cerebromicrovascular protective effects of NMN highlight the preventive and therapeutic potential of NAD^+ intermediates as effective interventions in patients at risk for vascular cognitive impairment (VCI).

1. Introduction

Maintenance of cerebral homeostasis requires a tightly-controlled supply of oxygen and nutrients as well as washout of harmful metabolites through uninterrupted cerebral blood flow (CBF), which represents 15% of cardiac output [1]. The human brain comprises only 2% of the body's mass, yet it accounts for 20% of the resting total body O_2 consumption. The brain has limited energy reserves and cerebral

* Corresponding author. Reynolds Oklahoma Center on Aging, Department of Geriatric Medicine University of Oklahoma Health Sciences Center 975 NE 10th Street, BRC 1311 Oklahoma City, OK 73104, USA.
E-mail address: zoltan-ungvari@ouhsc.edu (Z. Ungvari).

https://doi.org/10.1016/j.redox.2019.101192
Received 22 February 2019; Received in revised form 2 April 2019; Accepted 7 April 2019
Available online 10 April 2019

oxygen content can sustain unimpeded neuronal function for only a short time if CBF decreases [2]. Thus, during periods of intense neuronal activity there is a requirement for rapid adjustment of regional oxygen and glucose delivery to metabolic demand through spatially localized adaptive increases in CBF. This is ensured by an evolutionarily conserved physiological mechanism known as neurovascular coupling (NVC) or functional hyperemia [1]. The cellular mechanisms of NVC include release of vasodilator NO from the microvascular endothelium, in response to increased neuronal and astrocytic activation [3,4].

It is now increasingly recognized that (micro)vascular contributions to cognitive impairment and dementia (VCID) play a critical role in elderly patients [1]. There is growing evidence that NVC responses are compromised both in elderly subjects [5–8] and aged laboratory animals [4,9], which may importantly contribute to the age-related decline in higher cortical function, including cognition [10] and gait performance [11]. This concept is supported by recent findings that pharmacologically induced neurovascular dysfunction in mice mimics important aspects of age-related cognitive impairment [12]. Further, our recent studies demonstrate that rescue of NVC responses by treatment with the mitochondria-targeted antioxidative peptide SS-31 [13] or pharmacological SIRT1 activators [4,14] mitigates cognitive impairment in aged mice. These successful preclinical studies provide proof-of-concept that development of translationally relevant therapeutic interventions that target molecular/cellular mechanisms contributing to age-related neurovascular dysfunction is feasible for prevention/treatment of cognitive impairment in elderly patients [4].

NAD^+ is a rate-limiting co-substrate for sirtuin enzymes, which are key regulators of pro-survival pathways and mitochondrial function in the endothelial cells [15–18]. There is increasing evidence that with age cellular NAD^+ availability decreases [19,20], which is a critical driving force in aging processes. In support of this theory it was demonstrated that enhancing NAD^+ biosynthesis extends lifespan in lower organisms [21] and improves health-span in mouse models of aging [22]. There is particularly strong evidence that in aged mice enhancing NAD^+ biosynthesis by treatment with nicotinamide mononucleotide (NMN; a key NAD^+ intermediate) [23] reverses age-related dysfunction in multiple organs, including the eye [24], skeletal muscle [19] and peripheral arteries [15,25]. A key mechanism underlying the anti-aging action of NMN treatment is reversing age-related decline in mitochondrial function [24]. Although there is strong evidence that mitochondrial dysfunction and increased mitochondrial oxidative stress contribute to cardiovascular dysfunction [26–28] and neurovascular impairment in aging [13], the potential protective effects of NMN on the aged cerebral microvasculature and NVC responses have not been investigated.

The present study was designed to test the hypothesis that NMN supplementation can rescue neurovascular coupling responses in aged mice by attenuating mitochondrial oxidative stress in cerebromicrovascular endothelial cells. To achieve this goal, aged mice were treated with NMN for two weeks. Mice were behaviorally evaluated on a battery of tests for characterization of cognitive function and motor coordination, which are sensitive to alterations in NVC responses. Then, functional tests for NVC responses and cerebromicrovascular endothelial function were performed. Markers of oxidative stress and expression of genes regulating neurovascular coupling responses, antioxidant defenses and mitochondrial function were assessed. To substantiate the *in vivo* findings the effects of NMN on mitochondrial ROS production and mitochondrial bioenergetics in cerebromicrovascular endothelial cells derived from aged animals were obtained *in vitro*.

2. Material and methods

2.1. Animals, NMN supplementation

Young (3 month, n = 30) and aged (24 month, n = 40) male C57BL/6 mice were purchased from the aging colony maintained by the National Institute on Aging at Charles River Laboratories (Wilmington, MA). Animals were housed under specific pathogen-free barrier conditions in the Rodent Barrier Facility at University of Oklahoma Health Sciences Center under a controlled photoperiod (12 h light; 12 h dark) with unlimited access to water and were fed a standard AIN-93G diet (ad libitum). Mice in the aged cohort were assigned to two groups (n = 20 each group). One group of the aged mice was injected daily with NMN (i.p. injections of 500 mg NMN/kg body weight per day) or the equivalent volume of PBS for 14 consecutive days at 6 p.m. and 8 a.m. on day 14 and were sacrificed 4 h after last injection. Similar dosages of NMN has been shown to exert potent anti-aging effects on mouse health span [25]. All procedures were approved by the Institutional Animal Use and Care Committees of the University of Oklahoma Health Sciences Center. All animal experiments complied with the ARRIVE guidelines and were carried out in accordance with the National Institutes of Health guide for the care and use of Laboratory animals (NIH Publications No. 8023, revised 1978).

2.2. Behavioral studies

Previous studies suggest that alterations of neurovascular coupling responses associate with changes in cognition as well as sensory-motor function [12,29]. Thus, after the treatment period behavioral tasks were performed to characterize the effect of NMN supplementation on learning and memory, sensory-motor function, gait and locomotion (n = 20 in each group).

2.2.1. Radial arms water maze testing

Spatial memory and long term memory in each group of mice was tested by observing and recording escape latency, distance moved, and velocity during the time spend in the radial arms water maze as described [13,29]. The maze consisted of eight arms 9 cm wide that radiated out from an open central area, with a submerged escape platform located at the end of one of the arms. Paint was added into the water to make it opaque. The maze was surrounded by privacy blinds with extramaze visual cues. Intramaze visual cues were placed at the end of the arms. The mice were monitored by a video tracking system directly above the maze as they waded and parameters were measured using Ethovision software Noldus Information Technology Inc., Leesburg, VA, USA. Experimenters were unaware of the experimental conditions of the mice at the time of testing. During the learning period each day, mice were given the opportunity to learn the location of the submerged platform during two sessions each consisting of four consecutive acquisition trials. On each trial, the mouse was started in one arm not containing the platform and allowed to wade for up to one minute to find the escape platform. All mice spent 30 s on the platform following each trial before beginning the next trial. The platform was located in the same arm on each trial. Over the three days of training, mice in the young control group gradually improved performance as they learned the procedural aspects of the task. Upon entering an incorrect arm (all four paws within the distal half of the arm) or failing to select an arm after 15 s the mouse was charged an error. Learning capability was assessed by comparing performance on days 2 and 3 of the learning period.

2.2.2. Elevated plus maze learning protocol

Mice were also assessed for learning capacity using an elevated plus maze-based learning protocol as previously described [30]. A gray elevated plus maze apparatus was used. Two open arms (25 × 5 cm) and two (25 × 5 cm) closed arms were attached at right angles to a central platform (5 × 5 cm). The apparatus was 40 cm above the floor. Mice were placed individually at the end of an open arm with their back to the central platform. The time for mice to cross a line halfway along one of the closed arms was measured (transfer latency) on day 1 and day 2. Mice had to have their body and each paw on the other side of the line. If a mouse had not crossed the line after 120 s, it was placed

beyond it. After crossing the line, mice had 30 s for exploring the apparatus. Learning was defined as reduced transfer latency on day 2 compared to day 1. Higher relative difference in transfer latency on day 1 and day 2 indicates superior hippocampal function.

2.2.3. Novel object recognition test

The novel object recognition task was also performed to characterize the effect of NMN on learning and memory [12,31]. The results of the test are influenced by both hippocampal and cortical microvascular impairment. The test consists of a habituation phase, acquisition (familiarization) phase, and trial phase. During the habituation phase the animals explored the empty open-field arena for 5 min. Then, in the acquisition phase the mice explore two identical objects for 2 min. After a 4 h delay, a trial phase occurred. During this period animals explored the familiar object and a novel object for 2 min. Exploration of the objects was defined as directing the nose at a distance ≤2 cm to the object and/or touching it with the nose. For data collection and analysis Ethovision software (Noldus Information Technology Inc., Leesburg, VA, USA) was used. Sitting or climbing on it was not considered as an exploration. All objects used in this study were made of washable odorless plastic and were different in shapes and colors but identical in size. A percent of time spent exploring the novel object relative to the total time spent exploring both objects was used as a measure of novel object recognition. The Recognition Index (RI, representing the time spent investigating the novel object [T_{novel}] relative to the total object investigation) was used as the main index of retention, which was calculated according to the following formula: [$RI = T_{novel}/(T_{novel} + T_{familiar})$]. The arena and the objects were cleaned with 70% ethanol between the trials to prevent the existence of olfactory cues.

2.2.4. Rotarod performance

Motor coordination was assessed in each group of mice by using an automated four-lane rotarod (Columbus Instruments, Columbus, OH) as described [12]. In brief, mice were pre-trained by placing them on the moving rotarod at 10 r.p.m. until they performed at this speed for 120 s. On the day of testing, mice were habituated in their home cages and acclimate to the testing room for at least 15 min. The test phase consisted of 3 trials (separated by 15 min inter-trial intervals). The testing apparatus was set to accelerate from 4 to 40 r.p.m. in 300 s. One mouse was then placed on each lane and the rotarod was started with an initial rotation of 4 r.p.m. The rotational velocity was set to increase every 10 s and the latency to fall was recorded. Latency to fall was recorded in seconds by an infra-red beam across the fall path along with the max r.p.m. sustained by each mouse [32].

2.2.5. Grip strength test

A grip strength test was used to measure the maximal muscle strength of forelimbs of the mice [12]. Forelimb grip strength was assessed using a grip strength meter (Chatillon Ametek Force Measurement, Brooklyn, New York). The strength measurements of each group of mice were measured three times by the same investigator. The maximum grip strength values were used for subsequent analysis.

2.2.6. Analysis of gait function

To determine how aging and NMN treatment affect gait coordination, we tested the animals using an automated computer assisted method (CatWalk; Noldus Information Technology Inc. Leesburg, VA) as described [13,29,33]. Using the CatWalk system the detection of paw print size, pressure and pattern during volunteer running on an illuminated glass walkway by a camera placed under the glass surface provides an automated analysis of gait function and the spatial and temporal aspects of interlimb coordination [12,34]. Briefly, animals were trained to cross the walkway and then, in a dark and silent room (< 20 lux of illumination), animals were tested in three consecutive runs. Data were averaged across ten runs in which the animal maintained a constant speed across the walkway. After manual identification and labeling of each footprint, spatial and temporal indices of gait were calculated (including swing speed, cadence, regularity index, brake and propulsion phase duration, stand index, duty cycle; size-adjusted base of support, stride length and distance between ipsilateral prints; stride length and stride time coefficient of variance, interlimb couplings).

2.3. Measurement of neurovascular coupling responses and cerebral blood flow

After behavioral testing, mice in each group were anesthetized with isoflurane (4% induction and 1% maintenance), endotracheally intubated and ventilated (MousVent G500; Kent Scientific Co, Torrington, CT). A thermostatic heating pad (Kent Scientific Co, Torrington, CT) was used to maintain rectal temperature at 37 °C [4]. End-tidal CO_2 was controlled between 3.2% and 3.7% to keep blood gas values within the physiological range, as described [12,35]. The right femoral artery was canulated for arterial blood pressure measurement (Living Systems Instrumentations, Burlington, VT) [4]. The blood pressure was within the physiological range throughout the experiments (90–110 mmHg). Mice were immobilized and placed on a stereotaxic frame (Leica Microsystems, Buffalo Grove, IL) and the scalp and periosteum were pulled aside. Mice were equipped with an open cranial window and changes in CBF were assessed above the left barrel cortex using a laser Doppler probe (Transonic Systems Inc., Ithaca, NY), as described [4,12,35]. The cranial window was superfused with artificial cerebrospinal fluid (ACSF, composition: NaCl 119 mM, $NaHCO_3$ 26.2 mM, KCl 2.5 mM, NaH_2PO_4 1 mM, $MgCl_2$ 1.3 mM, glucose 10 mM, $CaCl_2$ 2.5 mM, pH = 7.3, 37 °C). The right whisker pad was stimulated by a bipolar stimulating electrode placed to the ramus infraorbitalis of the trigeminal nerve and into the masticatory muscles. The stimulation protocol used to investigate neurovascular coupling consisted of 10 stimulation presentation trials with an intertrial interval of 70 s, each delivering a 30-s train of electrical pulses (2 Hz, 0.2 mA, intensity, and 0.3 ms pulse width) to the mystacial pad after a 10-s prestimulation baseline period. Changes in CBF were averaged and expressed as percent (%) increase from the baseline value [36]. Experiments lasted ~20–30 min/mouse, which permitted stable physiological parameters to be obtained. To assess the role of NO mediation, CBF responses to whisker stimulation were repeated in the presence of the nitric oxide synthase inhibitor N^{ω}-Nitro-L-arginine methyl ester (L-NAME; 3×10^{-4} moL/L, 20 min). In separate experiments CBF responses to whisker stimulation were obtained before and after topical administration of the mitochondrial antioxidant mitoTEMPO (10^{-5} moL/L). To assess microvascular endothelial function, CBF responses to topical administration of acetylcholine (ACh; 10^{-5} moL/L) were obtained before and after topical administration of the mitochondrial antioxidant mitoTEMPO (10^{-5} moL/L).

Basal CBF was assessed in a separate cohort of control and experimental mice (n = 5 in each group) anesthetized with isoflurane using arterial spin labeling magnetic resonance imaging following published protocols [33].

In each study the experimenter was blinded to the treatment of the animals. At the end of the experiments the animals were transcardially perfused and decapitated. The brains were immediately removed and pieces of the somatosensory and motor cortex were isolated and frozen for subsequent analysis. All reagents used in this study were purchased from Sigma-Aldrich (St Louis, MO) unless otherwise indicated.

2.4. Assessment of the effect of NMN supplementation on markers of oxidative stress

To characterize the effect of NMN treatment on cellular redox homeostasis in aging, 3-nitrotyrosine (3-NT, a marker for peroxynitrite action) was assessed in homogenates of cortical samples using OxiSelect

Protein Nitrotyrosine ELISA Kits (Cell Biolabs), according to the manufacturer's guidelines, as previously described [4]. In the microcirculation of aged rodents endothelium-derived NO was shown to react with $O_2^{\cdot-}$ forming $ONOO^-$ thus decreasing the bioavailability of NO [37,38]. Previously we showed that aged mouse brains exhibit an increased 3-nitrotyrosine content [4], a biomarker of increased $ONOO^-$ formation, suggesting that impaired endothelial mediation of cerebromicrovascular dilation in aging is due to increased scavenging of vasodilator NO [9].

As an additional marker of oxidative stress, 8-isoprostane content in the cortical tissue was measured using the 8-isoprostane EIA kit (Cayman Chemical Company, Ann Arbor, MI) according to the manufacturer's guidelines as previously reported [4].

2.5. Assessment of endothelial function in the aorta

To assess the specific effect of NMN treatment on endothelial function, endothelium-dependent vasorelaxation was assessed in isolated aorta ring preparations as described previously [39]. In brief, aortas were cut into ring segments 1.5 mm in length and mounted in myographs chambers (Danish Myo Technology A/S, Inc., Denmark) for measurement of isometric tension. The vessels were superfused with Krebs buffer solution (118 mM NaCl, 4.7 mM KCl, 1.5 mM $CaCl_2$, 25 mM $NaHCO_3$, 1.1 mM $MgSO_4$, 1.2 mM KH_2PO_4, and 5.6 mM glucose; at 37 °C; gassed with 95% air and 5% CO_2). After an equilibration period of 1 h during which an optimal passive tension was applied to the rings (as determined from the vascular length-tension relationship), they were pre-contracted with 10^{-6} M phenylephrine and relaxation in response to acetylcholine was measured.

2.6. Assessment of vascular oxidative stress

To characterize vascular ROS production isolated segments of the aorta were loaded with the redox sensitive dye dihydroethidium (DHE, Invitrogen, Carlsbad CA; 3×10^{-6} moL/L; for 30 min) in oxygenated Krebs' solution (at 37 °C) as previously reported [34,39–42]. After loading the dye was washed out five times with warm Krebs buffer, and the vessels were allowed to equilibrate for another 20 min. Then, the vessels were embedded in OCT medium and cryosectioned. Confocal images were captured using a Leica SP2 confocal laser scanning microscope (Leica Microsystems GmbH, Wetzlar, Germany). Average nuclear DHE fluorescence intensities were assessed using the Metamorph software (Molecular Devices LLC, Sunnyvale, CA) and values for each animal in each group were averaged.

2.7. Measurement of vascular and endothelial NAD^+ levels

To confirm efficiency of NMN treatment, NAD^+ levels were measured in snap frozen aortas from young and aged mice using a bioluminescent assay (NAD/NADH-Glo Assay; Promega, Madison, WI), according to the manufacturer's instructions. Briefly, tissue was homogenized in PBS and lysed in a base solution with 1% DTAB. To measure the levels of the oxidized form, HCl was added to the solution and heated for 15 min at 60 °C. The luminescence signal was detected with a Tecan Infinite M200 plate reader. A similar protocol was followed for cultured endothelial cells (see below). Protein quantification was used for normalization purposes.

2.8. Establishment and characterization of primary CMVEC cultures

To evaluate the anti-aging action of NMN *in vitro*, we assessed the effects of NMN on cellular mtROS production and mitochondrial phenotype in cultured primary cerebromicrovascular endothelial cells (CMVECs). The establishment and characterization of the CMVEC strains used has been recently reported [4]. In brief, to establish primary cultures of CMVECs, the brains of male 3 and 24 month old F344xBN rats (obtained from the National Institute on Aging) were removed aseptically, rinsed in ice cold PBS and minced into ≈1 mm squares. The tissue was washed twice in ice cold 1X PBS by low-speed centrifugation (50 g, 2–3 min). The diced tissue was digested in a solution of collagenase (800U/g tissue), hyaluronidase (2.5U/g tissue) and elastase (3U/g tissue) in 1 ml PBS/100 mg tissue for 45 min at 37 °C in a rotating humid incubator. The digested tissue was passed through a 100 μm cell strainer. The single cell lysate was centrifuged for 2 min at 70 g. After removing the supernatant the pellet was washed twice in cold PBS supplemented with 2.5% fetal calf serum (FCS) and the suspension centrifuged at 300 g for 5 min at 4C. To create an endothelial cell enriched fraction the cell suspension was centrifuged using an OptiPrep gradient solution (Axi-Shield, PoC, Norway). Briefly, the cell pellet was resuspended in Hanks' balanced salt solution (HBSS) and mixed with 40% iodixanol thoroughly (final concentration: 17% (w/v) iodixanol solution; ρ = 1.096 g/ml). 2 ml of HBSS was layered on top and centrifuged at 400 *g* for 15 min at 20 °C. Endothelial cells, which banded at the interface between HBSS and the 17% iodixanol layer, were collected. The endothelial cell enriched fraction was incubated for 30 min at 4 °C in the dark with anti-CD31/PE (BD BD Biosciences, San Jose, CA, USA), anti-MCAM/FITC (BD Biosciences, San Jose, CA, USA). After washing the cells twice with MACS Buffer (Milltenyi Biotech, Cambridge, MA, USA) anti-FITC and anti-PE magnetic bead labeled secondary antibodies were used for 15 min at room temperature. Endothelial cells were collected by magnetic separation using the MACS LD magnetic separation columns according to the manufacturer's guidelines (Milltenyi Biotech, Cambridge, MA, USA). The endothelial fraction was cultured on fibronectin coated plates in Endothelial Growth Medium (Cell Application, San Diego, CA, USA) for 10 days. Endothelial cells were phenotypically characterized by flow cytometry (GUAVA 8HT, Merck Millipore, Billerica, MA, USA). Briefly, antibodies against five different endothelial specific markers were used (anti-CD31-PE, anti-erythropoietin receptor-APC, anti-VEGF R2-PerCP, anti-ICAM-fluorescein, anti-CD146-PE) and isotype specific antibody labeled fractions served as negative controls. Flow cytometric analysis showed that after the third cycle of immunomagnetic selection there were virtually no $CD31^-$, CD146-, EpoR- and VEGFR2-cells in the resultant cell populations. All antibodies were purchased from R&D Systems (R&D Systems, Minneapolis, MN, USA).

Primary CMVECs were cultured in custom-made Rat Brain Endothelial Cell Growth Medium (Cell Applications, Inc.) with reduced nicotinamide concentration (11.04 μM). Since the results of assays investigating mtROS, mitochondrial function and ATP concentration are affected by the number of viable cells, cell viability of each population was determined as described [43]. To assess the direct effects of NMN on endothelial mitochondrial function primary CMVECs derived from young and aged rats were treated with NMN (Santa Cruz, Dallas, TX) *in vitro* (5×10^{-4} moL/L; for 1–5 days).

2.9. SIRT1 and SIRT2 shRNA transfection

To determine the role of sirtuin signaling in the anti-aging endothelial effects of NMN treatment, the downregulation of SIRT1 and SIRT2, key anti-aging proteins whose activity is regulated by NAD levels, in CMVECs was achieved by RNA interference using proprietary, tested SIRT1 and SIRT2 short hairpin RNA (shRNA) sequences (GeneCopoeia, Rockville, MD). CMVECs were transfected using the electroporation-based Amaxa Nucleofector technology (Amaxa, Gaithersburg, MD), as we have previously reported [16,18]. Experiments were performed on day 2 after the transfection when gene silencing was optimal.

2.10. Measurement of mitochondrial ROS production and endothelial H_2O_2 and NO release

The assess the effect of NMN treatment on age-related

mitochondrial oxidative stress, mitochondrial production of ROS (mtROS) in CMVECs was measured using MitoSOX Red (Invitrogen/Thermo Fisher Scientific), a mitochondrion-specific hydroethidine-derivative fluorescent dye [27,28,44–48]. In brief, cells were incubated with MitoSox (5×10^{-6} moL/L; for 30 min, at 37 °C, in the dark). The cells were then washed with PBS and MitoSox fluorescence was measured by flow cytometry (GUAVA 8HT, Merck Millipore, Billerica, MA, USA).

In separate experiments, the effect of NMN treatment on age-related increases in cellular H_2O_2 production was measured fluorometrically in CMVECs using the Amplex red/horseish peroxidase assay as described [45]. The H_2O_2 generation rate was compared by measuring the time course of the buildup of resorufin fluorescence for 60 min by a Tecan Infinite M200 plate reader.

To assess the effect of NMN treatment on age-related decline in NO release, the production of NO in CMVECs was measured using the fluorescent indicator DAF-FM (4-amino-5-methylamino- 2′,7′-difluorescein; 5 μmoL/L for 30 min at 37 °C; Invitrogen/Thermo Fisher Scientific).

2.11. Measurement of mitochondrial membrane potential

To further elucidate the effects of NMN on mitochondrial function, we determined how it impacts mitochondrial membrane potential in CMVECs using the mitochondrial membrane potrential indicator fluorescent dye JC-1 (Guava Technologies, Hayward, CA). JC-1 is a cationic carbocyanine dye that accumulates in energized mitochondria. When it is present in its monomer form in the mitochondria at low concentrations (due to low mitochondrial potential), the dye exhibits green fluorescence. When it accumulates in the energized mitochondria and forms J-aggregates at higher concentrations (due to high mitochondrial potential), it exhibits red fluorescence. These characteristics render JC-1 a sensitive marker for mitochondrial membrane potential: a decrease in the aggregate red fluorescence and an increase in monomer green fluorescence is indicative of depolarization whereas an increase in the aggregate red fluorescence and a decrease in monomer green fluorescence is indicative of hyperpolarization. Cells were labeled with JC-1 for 30 min at 37 °C and fluorescence was analyzed with glow cytometry. The red/green fluorescence ratio was calculated as an indicator of mitochondrial membrane potential.

2.12. Mitochondrial bioenergetics assay

To substantiate the endothelium-protective effect of NMN, we performed real-time measurements of the oxygen consumption rate (OCR; a marker of oxidative phosphorylation) in young and aged CMVECs after treatment with NMN (5×10^{-4} mM NMN, for 5 days) using a Seahorse XF96 extracellular flux analyzer.

In brief, CMVECs were seeded into XF96 cell culture microplates in Seahorse XF-Assay media (Agilent Technologies) supplemented with 25 mM glucose and 1 mM sodium pyruvate (pH 7.4) the day before the assay. Plates were maintained for 45 min at 37 °C in 0% CO_2 prior to the measurement. Basal respiration, coupling efficiency, and spare respiratory capacity were compared using the Mito Stress Test Kit following the manufacturer's protocol. OCR was monitored before and after the addition of the electron transport inhibitors oligomycin (1.0 μM) and FCCP (1.0 μM), an ionophore that is a mobile ion carrier, and a mixture of antimycin-A (1.0 μM) (which is a complex III inhibitor) and rotenone (1.0 μM), a mitochondrial inhibitor that prevents the transfer of electrons from the Fe–S center in complex I to ubiquinone. Basal respiration (baseline respiration minus antimycin-A post injection respiration), ATP synthesis coupled respiration (baseline respiration minus oligomycin post injection respiration), maximal respiratory capacity (FCCP stimulated respiration minus antimycin-A post injection respiration) and reserve respiratory capacity (FCCP stimulated respiration minus baseline respiration) were calculated. Sample protein content was used for normalization purposes.

2.13. Quantification of ATP levels

To correlate these observed changes in OCR directly to ATP production, we also measured cellular ATP concentration in CMVECs. ATP levels in endothelial cells were assessed using the ENLITEN ATP bioluminescent assay (Promega) according to the manufacturer's instructions. Briefly, CMVEC were seeded in 96-well plates (for 24 h at 37 °C under 5% CO_2). For ATP determination the cells were homogenized in Passive Lysis Buffer (Promega). The samples were diluted 1:10 and mixed with an equal volume of the luciferase reagent. The plates were incubated at room temperature for 10 min and then the luminescence signal was detected with a Tecan Infinite M200 plate reader. ATP quantification was carried out from a standard curve using ATP disodium salt hydrate. BCA protein determination was performed for normalization purposes. Cell viability of each population was determined by flow cytometry (Guava easyCyte 8HT) to ensure similar viability of CMVECs in each group in a parallel experiment using the ViaCount Assay (Millipore).

2.14. Electron microscopy

Brains (n = 5 animals in each group) were perfusion fixed under 100 mmHg pressure using Karnowsky's method [49]. Thin sections were obtained with an ultramicrotome, stained with osmium tetroxide, and examined with a transmission electron microscope as previously described [50]. Mitochondrial volume densities were obtained in a blinded fashion using the principles of Weibel [51]. Data were expressed as relative changes in volume density (volume of mitochondria per cytoplasmic volume).

2.15. Measurement of mitochondrial DNA content in CMVECs

Total DNA was isolated from CMVECs using the QIAamp DNA Mini QIAcube Kit (QIAGEN). Mitochondrial DNA (mtDNA) copy number was determined by qPCR as described [17], using cytochrome oxidase III and β-actin as markers for the copy numbers of mtDNA and genomic DNA, respectively.

2.16. Quantitative real-time RT-PCR

A quantitative real time RT-PCR technique was used to analyze mRNA expression of genes relevant for neurovascular impairment and age-related mitochondrial dysfunction in cortical, cerebrovascular, aortic and endothelial samples using validated TaqMan probes (Applied Biosystems) and a Strategen MX3000 platform, as previously reported [4,35,52]. Targets included the nitric oxide synthases eNOS and nNOS (*Nos3* and *Nos1*, respectively), arginases (*Arg1, Arg2*; which regulate NO synthase activity and were proposed to contribute to endothelial dysfunction in aging [53]), antioxidant enzymes, enzymes involved in NAD metabolism and nuclear- and mitochondrion-encoded subunits of the electron transport chain. In brief, total RNA was isolated with a Mini RNA Isolation Kit (Zymo Research, Orange, CA) and was reverse transcribed using Superscript III RT (Invitrogen) as described previously [35]. Quantification was performed using the efficiency-corrected ΔΔCq method. The relative quantities of the reference genes *Hprt, Ywhaz, B2m*, *Actb* and S18 were determined and a normalization factor was calculated based on the geometric mean for internal normalization. Fidelity of the PCR reaction was determined by melting temperature analysis and visualization of the product on a 2% agarose gel.

2.17. Quantitative mass spectrometry analysis

Selective reaction monitoring (SRM) mass spectrometry was used to quantify vascular anti-oxidant protein expression, as previously

described [54]. For these assays, 60-μg amounts of aorta lysates were mixed with 8 pmol of bovine serum albumin (BSA) as an internal standard and 50 μl of 10% SDS. The samples were heated at 80 °C for 15 min before precipitating the proteins in 80% acetone overnight at −20 °C. The protein pellet was dissolved in 60 μl of sample buffer and a 20-μl aliquot containing 20 μg of protein run 1.5 cm into a 12.5% SDS-polyacrylamide gel. The gel was fixed and stained with GelCode Blue (Pierce). For each sample, the entire 1.5-cm lane was cut out of the gel and divided coarsely. The gel pieces were washed to remove the stain, reduced with DTT, alkylated with iodoacetamide, and digested with 1 μg of trypsin overnight at room temperature. The peptides produced in the digest were extracted with 50% methanol, 10% formic acid in water. The extract was evaporated to dryness and reconstituted in 150 μl of 1% acetic acid in water for analysis. The samples were analyzed using SRM with a triple quadrupole mass spectrometer (ThermoScientific TSQ Vantage) configured with a splitless capillary column HPLC system (Eksigent, Dublin, CA, USA). Samples (10 μl) were injected onto a 10 cm × 75 μm C18 capillary column (Phenomenex, Jupiter C18). The column was eluted at 160 nL/min with a 30-min linear gradient of acetonitrile in 0.1% formic acid. Data were processed by using Pinpoint to find and integrate the correct peptide chromatographic peaks. The response for each protein was taken as the total response for all peptides monitored. To quantify protein expression, the relative abundance of each protein was first normalized to the BSA internal standard and then normalized to the geometric mean of cellular reference proteins [54].

2.18. Statistical analysis

Statistical analysis was carried out by one-way ANOVA followed by Tukey's post hoc test or unpaired *t*-test, as appropriate. Dose-response curves for vascular relaxations were analyzed by two-way ANOVA for repeated measures followed by Bonferroni multiple comparison test. A p value less than 0.05 was considered statistically significant. Data are expressed as mean ± S.E.M.

3. Results

3.1. NMN supplementation rescues NVC responses in aged mice by restoring endothelial NO mediation

CBF responses in the whisker barrel cortex elicited by contralateral whisker stimulation were significantly decreased in aged mice compared to young animals indicating impaired NVC in aging (representative CBF tracings are shown in Fig. 1A, summary data are shown in Fig. 1B) [9]. We found that a 14-day treatment with NMN significantly increased CBF responses induced by contralateral whisker stimulation in aged mice, restoring NVC to levels observed in young mice (Fig. 1A–B). Further, perfusion mapping of cerebral coronal slices in each group of animals was performed by MRI. We found that basal CBF was decreased in aged mice as compared to young animals. NMN treatment significantly increased CBF in aged mice (Supplemental Fig. S1).

There is strong experimental evidence, obtained using both pharmacological inhibitors and genetically modified animals, that NO production by the microvascular endothelium plays a critical role in NVC responses and that cerebromicrovascular endothelial dysfunction significantly contributes to age-related neurovascular uncoupling [3,4]. Accordingly, in untreated aged animals administration of the NO synthase inhibitor L-NAME was without effect, whereas in young mice it significantly decreased NVC responses, eliminating the differences between the age groups (Fig. 1B). In NMN treated aged mice L-NAME significantly decreased CBF responses elicited by whisker stimulation (Fig. 1B), suggesting that NMN treatment restored the NO mediation of NVC in aged animals. To further ascertain the endothelial protective effects of NMN supplementation, endothelium-dependent vasodilator responses to acetylcholine were tested. In young mice topical administration of acetylcholine resulted in significant CBF increases, whereas these responses were significantly attenuated in aging mice. Treatment of aged mice with NMN significantly improved acetylcholine-induced vasodilation (Fig. 1C).

Previously we found that treatment with the mitochondria-targeted antioxidative peptide SS-31 can improve both NVC responses and acetylcholine-induced vasodilation in the brains of aged mice [13]. Our results showing that treatment with MitoTEMPO also restores NVC responses and acetylcholine-induced responses in aged mice extend these findings (Supplemental Fig. S2). Similar findings were obtained in isolated aorta ring preparations from aged mice supplemented with NMN (Fig. 1E). To assess the role of endothelium-derived NO, L-NAME was applied. L-NAME significantly inhibited acetylcholine-induced vasorelaxation, eliminating the differences between the three groups. These finding suggests that NMN significantly improves endothelial function by restoring endothelial NO mediation in aged vessels, extending recent findings [25]. Efficiency of NMN treatment was confirmed by demonstration of increased vascular NAD^+ levels (Fig. 1F). NMN treatment attenuated age-related increases in oxidative/nitrosative stress, as indicated by the reduced tissue 3-nitrotyrosine (Fig. 1D) and isoprostane (Supplemental Fig. S3, panel A) levels and vascular DHE staining (Supplemental Fig. S3, panel B), whereas it did not affect mRNA and protein expression of NO synthases or antioxidant enzymes (Supplemental Figs. S4 and S5, respectively). The effects of aging on expression of *Nmnat1, Nmnat3* and *Nampt* in cerebral vessels and aortas are shown in Supplemental Fig. S6 panels A and B.

3.2. NMN attenuates mitochondrial oxidative stress and improves mitochondrial bioenergetics in aged cerebromicrovascular endothelial cells

To substantiate the endothelial protective effects of NMN *in vitro*, we assessed the effects of NMN on cellular mtROS production in cultured primary cerebromicrovascular endothelial cells (CMVECs) derived from aged animals using the MitoSox fluorescence method. First we demonstrated that in aged CMVECs NAD^+ content was significantly decreased, whereas it was normalized by treatment with NMN (Fig. 2A). We found that in aged CMVECs mtROS production was significantly increased as compared to that in CMVECs derived from young animals (Fig. 2B and C), which associated with a decreased production of NO (DAF fluorescence; Fig. 2D) as well as impaired mitochondrial membrane potential (Fig. 2E), and decreased ATP levels (Fig. 2F). NMN treatment attenuated mtROS generation (Fig. 2B and C), increased NO production (Fig. 2D), rescued mitochondrial membrane potential (Fig. 2E) and restored cellular ATP content (Fig. 2E) in aged CMVECs, eliminating the difference between the two age groups. NMN treatment also attenuated increased H_2O_2 release from aged CMVECs as measured by the Amplex Red assay (Supplemental Fig. S7). Attenuation of mtROS production in NMN-treated aged CMVECs was associated with significant improvement of both basal and maximal mitochondrial respiration (Fig. 2G–H). Combined shRNA knockdown of SIRT1/SIRT2 prevented the beneficial effects of NMN on mtROS (Fig. 2C), NO production (Fig. 2D), mitochondrial membrane potential (Fig. 2E) and mitochondrial respiration (Fig. 2H) in aged CMVECs. The effects of aging on expression of *Nmnat1, Nmnat3* and *Nampt* in CMVECs are shown in Supplemental Fig. S6 panel C.

3.3. NMN reverses age-related decline in mitochondrially encoded genes without promoting mitochondrial biogenesis

We could exclude that mitochondrial protective effects of NMN are linked to promotion of mitochondrial biogenesis. Using electron microscopy and unbiased morphometric methods we found that mitochondrial volume density in endothelial cells in the cerebral microcirculation was unaffected by NMN treatment (Fig. 3A–D). NMN treatment of aged mice also does not affect mtDNA content in cerebral

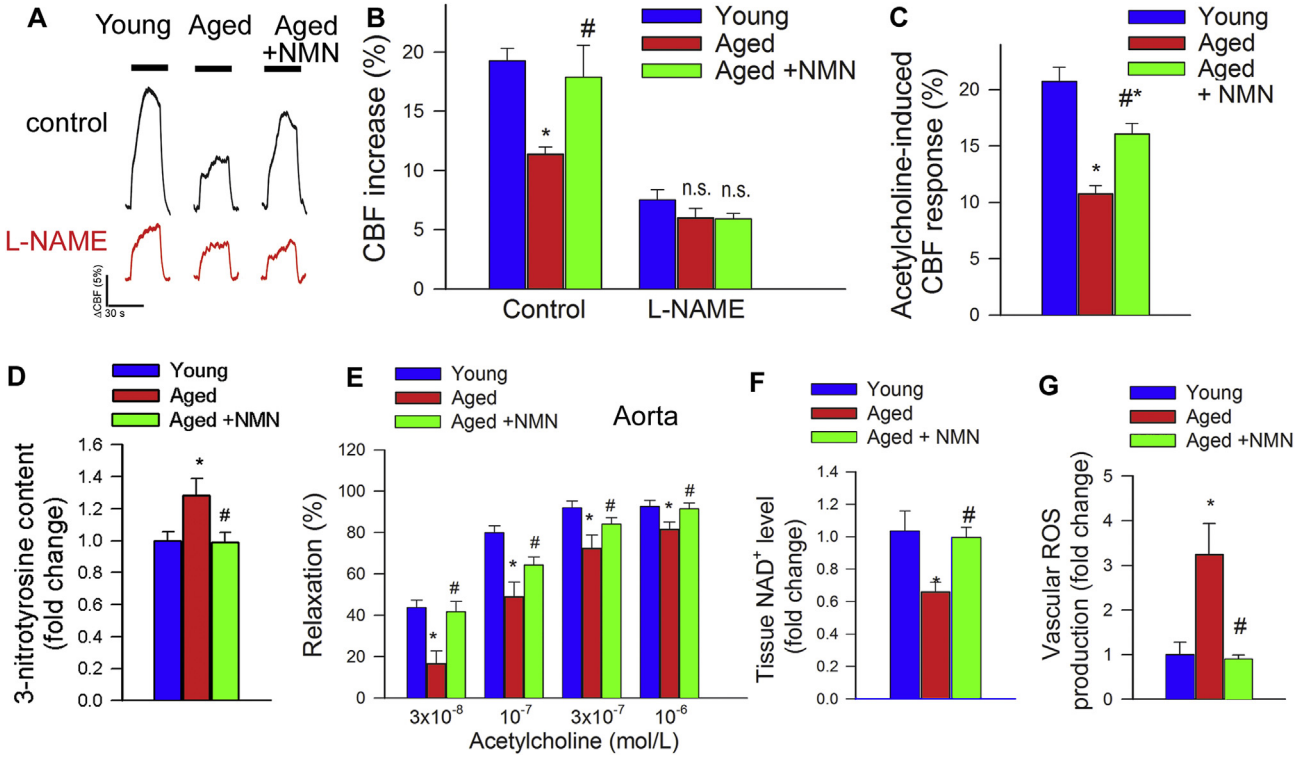

Fig. 1. NMN supplementation improves microvascular endothelial function and rescues NO mediation of neurovascular coupling responses in aged mice. A) Representative traces of cerebral blood flow (CBF; measured with a laser Doppler probe above the whisker barrel cortex) during contralateral whisker stimulation (30 s, 5 Hz) in the absence and presence of the NO synthase inhibitor L-NAME in young (3 month old), aged (24 month old) and NMN treated aged mice. B) Summary data showing that in aged mice NMN supplementation restores NO mediated component of NVC responses. C) In aged mice NMN supplementation improves endothelium-mediated CBF responses elicited by topical perfusion of acetylcholine. D) NMN supplementation decreases protein 3-nitrotyrosine content in the aged cortex, indicating decreased peroxynitrite formation. E-G) In aged mouse aortas NMN supplementation rescues acetylcholine-induced endothelium-mediated relaxation (E), increases tissue NAD^+ levels (F) and attenuates oxidative stress (G; see Methods). Data are mean ± S.E.M. (n = 5–8 for each data point).*P < 0.05 vs. Young; $^{\#}$P < 0.05 vs. Aged. (one-way ANOVA with post-hoc Tukey's test). n.s.: not significant.

arteries (Fig. 3E). Findings obtained in cultured CMVECs showing unaltered mtDNA content after NMN treatment extend the *in vivo* data (Fig. 3F).

Previous studies suggest that age-related decline in oxidative phosphorylation may be due to the specific loss of mitochondrially encoded transcripts [19]. Accordingly, we found that in aged cerebral arteries (Fig. 3G) and aged CMVECs (Supplemental Fig. S8) mRNA expression of mitochondrially encoded components of the electron transport chain was significantly decreased as compared to young ones, whereas those encoded by the nuclear genome remained unchanged with age (Supplemental Fig. S9). Importantly, NMN supplementation partially rescues age-related decreases in mRNA expression of mitochondrially encoded subunits of the electron transport chain both in cerebral arteries (Fig. 3G) and CMVECs (Supplemental Fig. S8).

3.4. Restoration of cerebromicrovascular function is associated with improved cognitive function in aged mice treated with NMN

Recently we demonstrated that specific, pharmacologically-induced neurovascular un-coupling results in detectable cognitive impairment [12]. To determine how rescue of cerebromicrovascular function by NMN supplementation impacts cognitive performance in aged mice, animals were tested in the radial arms water maze (Fig. 4A). We compared the learning performance of mice in each experimental group by analyzing the day-to-day changes in the combined error rate, working memory errors, successful escape rate, path length and time latency. During acquisition, mice from all groups showed a decrease in the combined error rate (Fig. 4B) across days, indicating learning of the task. After the first day of learning young mice consistently had lower combined error rate than aged mice (Fig. 4B). Decreases in the combined error rate induced by NMN supplementation in aged mice reached statistical significance by trial block 6.

To analyze working memory function (short-term memory that is involved in immediate conscious perception) we examined re-entries into incorrect arms (without hidden platform) that were previously attempted for escape. We found that working memory function was impaired in aged mice as compared to young controls (Fig. 4C). Aged mice with NMN supplementation showed significant restoration of working memory to levels comparable to young animals (Fig. 4C). NMN treatment thus resulted in complete behavioral rescue of working memory.

Successful escape rate from the maze was assessed by measuring the percent of animals that could find the hidden platform within the 60 s allowed for each trial. During acquisition, mice from all groups showed an increase in successful escape rate consistent with the learning of the task. Young mice exhibited significantly better escape success than untreated aged mice (Fig. 4D). Although in aged mice NMN treatment tended to increase the successful escape rate, the differences did not reach statistical significance (Fig. 4D).

We also compared path length (i.e. the distance that the mouse swam between maze entry and successful escape through the hidden platform) and escape latency (i.e. the time elapsed between entry and successful escape). During acquisition, mice from all groups displayed shorter path length (Fig. 4E) and lower escape latencies (Fig. 4F), indicating spatial learning. Young mice exhibited shorter path length (Fig. 4E) and lower escape latency (Fig. 4F) than untreated aged mice, which differences became pronounced by day 3. In aged mice NMN supplementation did not affect significantly either path length and

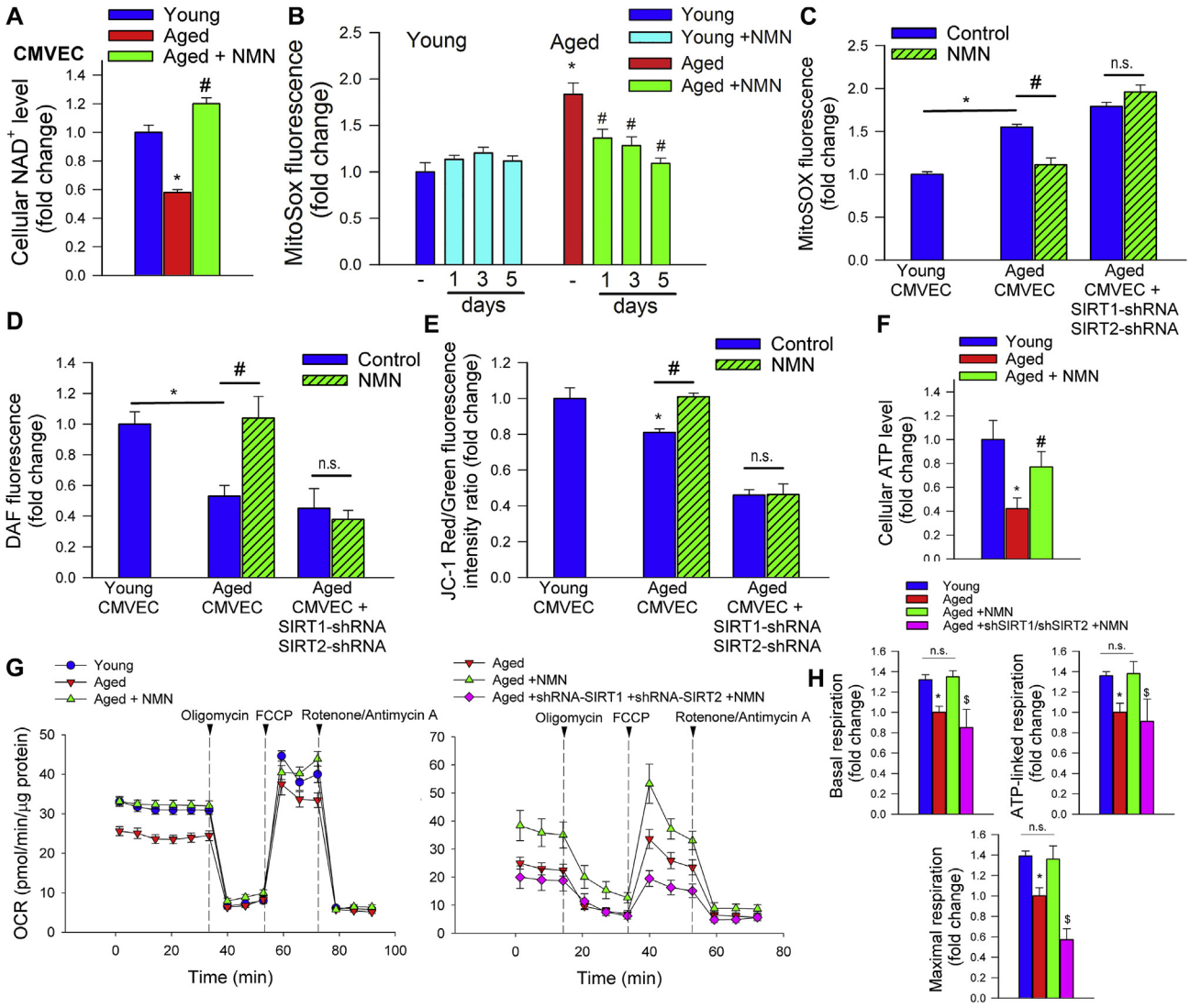

Fig. 2. Treatment with NMN improves mitochondrial energetics and attenuates mitochondrial ROS production in aged cerebromicrovascular endothelial cells (CMVECs). A) Treatment with NMN (5×10^{-4} moL/L; for 5 days) restores NAD^+ levels in primary CMVECs derived from aged rats. B) Treatment with NMN (5×10^{-4} moL/L; for 1–5 days) attenuates age-related increases in mtROS production in CMVECs (MitoSox fluorescence, assessed by flow cytometry). C) shRNA knockdown of SIRT1/SIRT2 prevents NMN-induced attenuation of mtROS in aged CMVECs. D-E) Treatment of aged CMVECs with NMN rescues cellular NO production (D; DAF fluorescence, assessed by flow cytometry) and increases mitochondrial membrane potential (E; JC-1 mitochondrial membrane potential probe) to levels observed in young cells. shRNA knockdown of SIRT1/SIRT2 prevents the NMN effect. F) Treatment of aged CMVECs with NMN restores cellular ATP levels. Data are mean ± S.E.M (n = 5–10 for each data point in A-F). *P < 0.05 vs. Young; #P < 0.05 vs. Aged. G) Attenuation of mtROS production and improved mitochondrial membrane potential in NMN treated aged CMVECs were associated with significant improvement of cellular oxygen consumption rate (OCR; a marker of oxidative phosphorylation; measured using the Seahorse XFe96 analyzer). Vertical dashed lines indicate assay drug injections. OCR in untreated young and aged CMVECs is shown for reference. Note the marked NMN-induced increase in both basal and maximal respiration in aged CMVECs. Right panel shows the effects of shRNA knockdown of SIRT1/SIRT2 on NMN-induced changes in OCR in aged CMVECs. OCR in aged CMVECs transfected with scrambled shRNA is shown for reference. H) Summary data showing the effects of aging and NMN on basal respiration, ATP-linked respiration and maximal respiration. Data are mean ± S.E.M., n = 9 for each data point.*P < 0.05 vs. Young; #P < 0.05 vs. Aged. $ P < 0.05 vs. Aged + NMN (one-way ANOVA with post-hoc Tukey's test). n.s.: not significant.

escape latencies. The analyses of noncognitive parameters revealed a slight age-related decline in swimming speed and an age-dependent increase in non-exploratory behavior (the cumulative time the mice spent not actively looking for the platform, e.g. floating), which were partially normalized toward young control levels by NMN treatment (Fig. 4G and H).

We also evaluated hippocampal-dependent learning and memory employing the elevated plus-maze. For young mice, transfer latency on day 2 was significantly decreased (by ~49%) compared to day 1 (Fig. 5A), indicating an intact learning effect. In contrast, for aged mice the transfer latency on day 1 and day 2 were similar, indicating impaired learning capability. NMN supplementation in aged mice restored learning performance to youthful levels (Fig. 5A).

Subsequently we also tested the performance of the mice in the novel object recognition test. We found no significant difference in the time that mice from each group spent exploring the two identical objects placed at the opposite ends of the arena during the acquisition phase, confirming that the location of the objects did not affect the exploration behavior of mice. In the trial phase with two different objects (one novel, the other familiar), young mice explored the novel object for a significantly longer time period, indicating their memory for the familiar object (Fig. 5B). In contrast, aged mice had a significantly lower calculated Recognition Index (RI). NMN supplementation in aged mice significantly improved their performance,

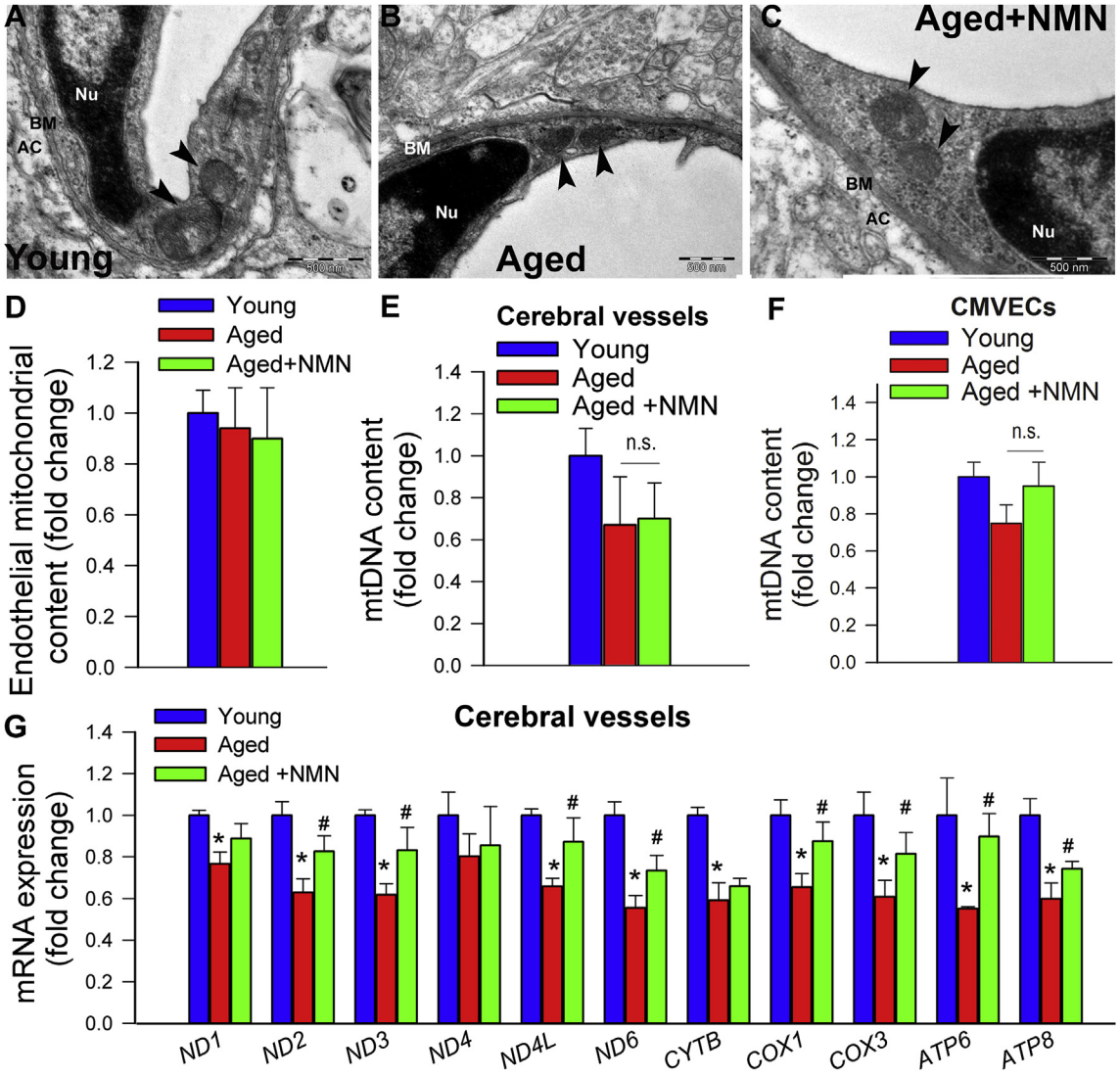

Fig. 3. Treatment with NMN rescues age-related downregulation of mitochondrially encoded subunits of the electron transport chain without promoting mitochondrial biogenesis. A-C) Representative electronmicrographs showing mitochondria in cerebromicrovascular endothelial cells in young (A), aged (B) and NMN treated aged mice (C); (arrowheads, mitochondria; nu, nucleus; bm, basal lamina; AC, astrocyte; scale bar: 500 nm). D) Summary data showing that NMN treatment does not affect mitochondrial volume density in aged cerebromicrovascular endothelial cells. E) NMN treatment of aged mice does affect mtDNA content in cerebral arteries. F) NMN treatment (5×10^{-4} moL/L; for 5 days) of aged CMVECs does not affect mtDNA content. G) NMN supplementation rescues age-related decreases in mRNA expression of mitochondrially encoded subunits of the electron transport chain in cerebral arteries. Data are mean ± SEM (n = 5–6 for each data point in D-G). *P < 0.05 vs. Young; #P < 0.05 vs. Aged. (one-way ANOVA with post-hoc Tukey's test). n.s.: not significant.

which is consistent with an improved hippocampal- and cortical-dependent recognition memory (Fig. 5B).

3.5. NMN supplementation improves gait performance in aged mice

To investigate the effects of age and NMN treatment on the motor performance of mice we measured performance of the accelerating rotarod and grip strength which evaluate muscle strength, balance, and endurance. NMN supplementation did not affect significantly age-related decreases in latency to fall from the rotarod (Fig. 5C) and did not reverse age-related decline in grip strength (Supplemental Fig. S10).

Age-related deficiencies in NVC responses in human patients [11] and animal models of aging [29] have been linked to gait abnormalities. Recent studies also demonstrate that pharmacologically-induced neurovascular uncoupling associates with subclinical gait alterations in mice [33]. To identify age- and treatment-related systematic differences between mouse gait patterns, principal component analysis (PCA) was carried out on the correlation matrix of spatial and temporal indices of gait. This analysis identified three principal components that accounted for ~63% of the variance in the data. We plotted the position of each mouse against the PC1, PC2, and PC3 axis in three-dimensional space (Fig. 5D). The most conspicuous trend was that aged and young mice were well separated along the PC1 axis, whereas NMN treated aged mice were clustered together with young mice. Collectively, the aforementioned results support the view that rescue of NVC by NMN treatment is associated with improved gait performance in aged mice. Selected individual gait parameters are shown in Supplemental Fig. S11.

4. Discussion

The key finding of this study is that short-term treatment with the NAD^+ precursor NMN rescues NVC responses and improves higher brain functions in a mouse model of aging that recapitulates key aspects of cerebromicrovascular dysfunction and cognitive deficit manifested in elderly patients.

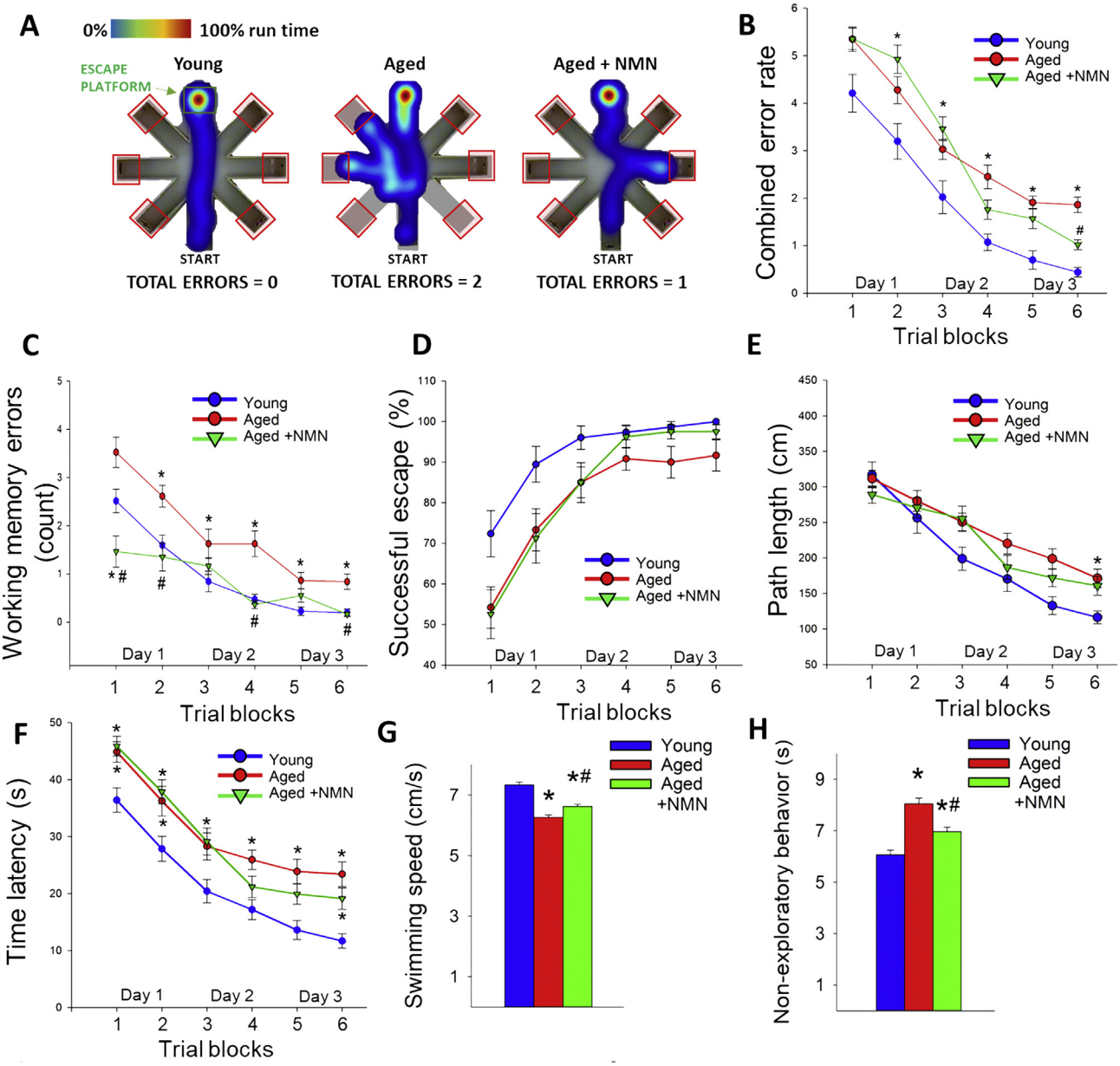

Fig. 4. In NMN treated aged mice rescue of neurovascular coupling responses associates with improved performance in the radial-arm water maze (RAWM). Young (3 month old), aged (24 month old) and NMN treated aged mice were tested in the RAWM. A) Heatmap representing the percentage of time spent in different locations in the maze for a randomly selected animal from each group during experimental day 3. Note that the untreated aged mouse required a greater amount of time and a longer path length in order to find the hidden escape platform. Older mice also re-enter a previously visited arm multiple time, accruing working memory errors. B) Older animals have higher combined error rates throughout day 2 and 3 of the learning phase. Combined error rate is calculated by adding 1 error for each incorrect arm entry as well as for every 15 s spent not exploring the arms. C) Older animals make significantly more working memory errors (repetitive incorrect arm entries) as compared to young mice. In contrast, aged mice treated with NMN perform this task significantly better than untreated aged mice. D) The ratio of successful escapes, averaged across trial blocks, is shown for each group. Note day-to-day improvement in the performance of young mice, which was significantly delayed in aged mice. Although aged mice treated with NMN tended to be more successful at finding the hidden escape platform in comparison to untreated age-matched controls, the difference did not reach statistical significance. Average path length (Panel E) and escape latencies (Panel F) required to reach the hidden platform in the RAWM for trial blocks 1–6. Young mice find the hidden platform sooner while swimming significantly less than aged animals. In aged mice treated with NMN the escape latencies and the average path length required to reach the hidden platform did not differ from that in aged mice. G) NMN had only marginal effect on the swimming speed. H) Aged control mice exhibited longer non-exploratory behavior compared to young mice. Treatment with NMN partially reduces the non-exploratory time to young levels. All data are shown as mean ± SEM. (n = 20 for each data point).

Elucidating the mechanisms by which aging impairs NVC responses is critical for the development of new targets and effective therapies for VCI. Here we show for the first time that NMN supplementation rescues NO mediation of NVC in aged mice supporting the concept that its potent cerebromicrovascular endothelial protective effects contribute significantly to its anti-aging, neuroprotective action. Additional evidence in support of this concept comes from the observations that NMN treatment restores NO release in aged CMVECs *in vitro* and that NMN supplementation also rescues endothelial NO-mediated vasodilation in the aortas of aged mice. Importantly, endothelium-derived NO plays versatile biological roles in addition to its role in vasoregulation. It is a paracrine regulator of cellular metabolism and mitochondrial function, it modulates the function of dozens of proteins by promoting nitrosylation on their cystine residues, it inhibits platelet aggregation,

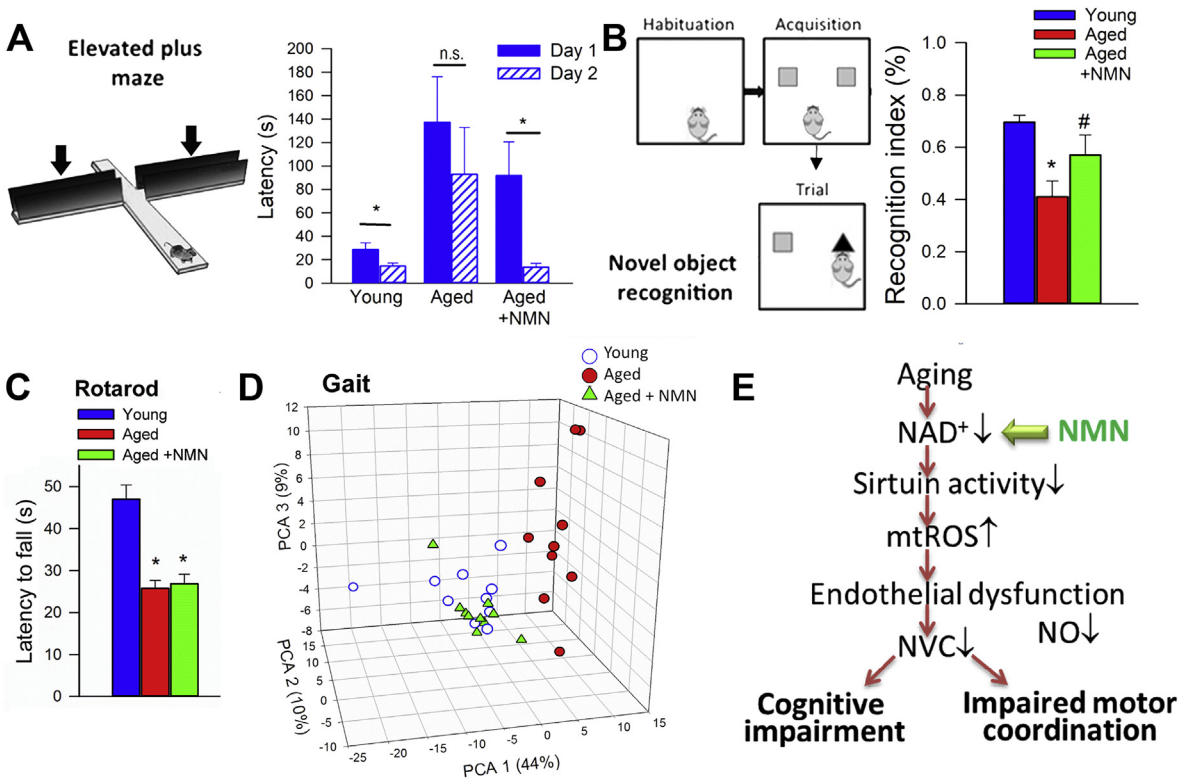

Fig. 5. In NMN treated aged mice rescue of neurovascular coupling responses associates with improved cognitive performance. A) NMN treatment improved learning ability in aged mice, as assessed using the elevated plus maze-based learning protocol (see Methods section). For young mice, transfer latency on day 2 was significantly decreased compared to day 1, indicating an intact learning effect. For aged mice the transfer latency on day 1 and day 2 were similar, indicating impaired learning capability. NMN supplementation in aged mice restored learning performance to youthful levels. B) NMN treatment restored recognition memory in aged mice as measured by the novel object recognition test (see Methods). Recognition memory is expressed as a recognition index which is defined as the ratio of time spent exploring the novel object over the total time spent exploring both familiar and novel objects. C) NMN supplementation in aged mice does not affect mean latencies to fall from the rotarod. All data are shown as mean ± SEM. (n = 20 for each data point). Statistical significance was calculated using one-way ANOVA with Tukey's post hoc test to determine differences among groups. *P < 0.05 vs. Young; #P < 0.05 vs. Aged control. D) NMN supplementation improves gait performance in aged mice. Shown is the 3D triplot of first three principal components (PC) identified by PCA on the correlation matrix of spatial and temporal indices of gait. Each point represents an individual mouse. Note, that mice in the same age groups clustered together. Differences between young and aged mouse gait were evident. NMN supplementation partially reverses age-related changes in mouse gait (MANOVA; P < 0.01 Aged vs. Aged treated; P < 0.01 Young vs. Aged). E) Scheme showing proposed role for increased NAD^+ deficiency and mitochondrial oxidative stress in cerebromicrovascular endothelial impairment and neurovascular dysfunction in aging and their pathophysiological consequences.

smooth muscle cell proliferation and leukocyte adhesion, promotes stability of atherosclerotic plaques and exerts potent anti-inflammatory, anti-apoptotic and pro-angiogenic effects. In that regard it is significant that NMN treatment was also shown to increase capillary density in the skeletal muscle [15]. Thus, rescue of cerebromicrovascular NO bioavailability by treatment with NAD precursors likely has clinical significance beyond restoration of NVC responses, potentially exerting diverse protective effects both on the cerebral vasculature and physiological function of other cell types, including neurons, astrocytes and microglia. The mechanisms underlying age-related decline in NAD^+ in endothelial cells are likely multifaceted and may include down-regulation of NAMPT (which catalyzes the rate limiting step in the biosynthesis of NAD^+) and increased utilization of NAD^+ by activated PARP-1 [55]. Thus, it is possible that combination treatments that simultaneously increase NAD production and inhibit its degradation (e.g. NMN plus a PARP-1 inhibitor) may offer additional benefits for neurovascular protection.

Our studies are the first to demonstrate that NMN treatment effectively attenuates age-related mitochondrial oxidative stress in cerebomicrovascular endothelial cells, suggesting a key role for this mechanism in NAD^+-mediated endothelial protection. In support of this concept using structurally different inhibitors/scavengers of mtROS production, including SS-31[13], resveratrol [4,45] and mitoTEMPO, we have demonstrated that age-related mitochondrial oxidative stress plays a central role in impaired NO mediation of NVC responses in aging. Recovery of endothelial function in aged peripheral arteries has also been reported using the SS-31[13], resveratrol [39] and MitoQ [56]. The mechanisms contributing to mitochondrial oxidative stress in the aged endothelium, which are affected by NMN treatment, are likely multifaceted and involve a dysfunctional electron transport chain. Reduced electron flow through the electron transport chain, in particular due to age-related dysfunction of complex I and complex III [57], likely increases electron leak and favors mtROS production. It is believed that dysregulation of mtDNA-encoded subunits of these complexes contribute to their age-related dysfunction. Increases in NAD^+ levels induced by NMN treatment were shown to activate SIRT1 [19], which regulates the expression of mtDNA-encoded subunits of the ETC [19]. Importantly, our results suggest that disruption of sirtuin signaling prevents NMN-induced mitochondrial protection and attenuation of mtROS production in aged CMVECs. Importantly, pharmacological sirtuin activators were also shown to attenuate mtROS and improve endothelial function in aged animals [58]. On the basis of the aforementioned findings and the data available in the literature [15,19] we speculate that increased sirtuin activation elicited by increased NAD^+ levels restores expression of mtDNA-encoded subunits, improving efficiency of the ETC, restoring bioenergetics and attenuating mtROS production. In addition, increased NAD^+:NADH ratio itself may also contribute to the reduction of mitochondrial oxidative stress [59],

whereas alterations in cellular and mitochondrial expression of antioxidant enzymes appear less important. Other mitochondrial factors affecting mtROS levels that may be potentially affected by sirtuin-regulated pathways include the mitochondrial Nox4-containing NADPH-oxidase, p66shc, as well as the ratios of reduced/oxidized co-factors (NAD(P)H, GSH) and thiol groups of proteins, that act as a mitochondrial redox buffer [26,59]. These factors should be investigated in future studies.

We find that restoration of NAD^+ levels by NMN treatment, in addition to reducing ROS generation, increases mitochondrial membrane potential and improves mitochondrial respiration in CMVECs in a sirtuin-dependent manner. We posit that sirtuin-mediated increases in mitochondrial membrane potential drives increased ATP production in NMN treated CMVECs. Such a mechanism is likely also operational in the cerebral microcirculation of NMN treated aged mice. In addition to sirtuin-mediated effects, because mitochondrial ATP production and membrane potential require NAD as an essential coenzyme, restoring an optimal NAD/NADH ratio itself should also promote efficient mitochondrial metabolism.

Normalization of mitochondrial membrane potential and increased efficiency of ATP generation likely also improve cellular functions independent of decreasing mtROS. For example, the microvascular endothelium in the brain, which maintains the blood-brain-barrier and exhibits controlled transcellular transport systems, has high energy demands. Future studies should determine how restoration of cellular energetics by NMN supplementation impacts barrier and transport function in capillaries in the aged brain. Interestingly, both NMN and the related NAD precursor nicotinamide riboside have recently been shown to improve neuronal mitochondrial function and behavioral phenotypes in models of neurodegenerative disease [60,61,62], suggesting that the net benefit *in vivo* could reflect effects on multiple distinct cell types within the brain. Astrocytic end feet also contain significant amounts of mitochondria. We predict that NMN treatment of aged mice may also exert beneficial effects on astrocytic functions that are affected by impaired mitochondrial energy metabolism and/or increased mtROS, including astrocytic contributions to NVC responses (e.g. release of ATP upon neuronal stimulation). This possibility should be tested in future studies.

There is a growing evidence from clinical [10,11] and experimental [12] studies that impairment of NVC responses contributes to the age-related decline in higher cortical functions. Restoration of this key homeostatic mechanism matching energy supply with the needs of active neuronal tissue is expected to exert beneficial effects on brain function in aging. The present study is the first to demonstrate that rescue of NVC by NMN supplementation in aging is associated with improvement of multiple domains of brain function, including hippocampal encoded memory functions. These results extend the findings of our previous studies demonstrating that rescue of NVC responses in aged mice by treatment with the mtROS inhibitors resveratrol [4] and SS-31 [13] is also associated with significant cognitive benefit [14]. In previous studies NMN supplementation was shown to improve health of obese aged mice [63]. Because there is strong evidence that aging and obesity exerts synergistic deleterious effects on NVC responses and mouse cognition [64], further studies are warranted to evaluate the potential benefits of NMN treatment on these endpoints in mouse models of geriatric obesity as well.

Neurovascular dysfunction in older adults [11] as well as in animal models of aging [29] has been linked to gait alterations. Recent experimental studies in mouse models of pharmacologically-induced neurovascular uncoupling established a mechanistic link between impaired NVC responses and gait abnormalities [12]. The present study extends these findings showing that rescue of NVC responses by NMN supplementation reverses age-related alterations in gait performance in mice. Gait dysfunction in geriatric patients is a major cause of functional impairment, contributes to falls and predicts increased risk of institutionalization and mortality. Identification of interventions targeting the cerebral microvasculature that can improve gait function in aging has great relevance for maintaining functional independence in late life and preventing falls.

4.1. Limitations of the study

A number of important limitations of the present study need to be considered. First, DHE is not specific to superoxide and is more considered a semi-quantitative assay. Also, the DAF assay is not specific to NO as it can also react with oxidation products of NO. Recent reports suggest that hydrogen sulfide can reverse aging-induced vascular alterations and promote NO synthesis, at least in part, by augmenting the effects NAD precursors [15,65,66]. Further studies are warranted to elucidate the interaction of hydrogen sulfide and NAD-dependent pathways as well as the role of reactive sulfur species in the aged cerebral microcirculation. We acknowledge as a limitation of the study that we could measure NAD + levels and ROS production only in the aorta.

5. Conclusions

In conclusion, our findings show that NMN supplementation exerts significant cerebromicrovascular protective effects in aged mice. NMN treatment attenuates endothelial oxidative stress, improves endothelial function and rescues NVC responses in the aged cortex, which likely contributes to improvement of higher cortical function (Fig. 5E). Our findings, taken together with the results of earlier studies [15,19,23,24], point to benefits at several levels of cerebrovascular and systemic pathology of aging and to the potential use of NMN as therapy for prevention of aging-induced vascular cognitive impairment. Importantly, NVC is compromised both in patients with Alzheimer's disease (AD) and in mouse models of AD, which is believed to accelerate clinical deterioration [1]. Thus, our findings are likely relevant to the treatment of AD in elderly patients as well. In laboratory animals long-term intake of NMN is well-tolerated without side effects [24] and clinical trials have been already started to assess the tolerability of NMN in humans [67] to develop it as an anti-aging nutraceutical. Thus, future clinical trials with NMN supplementation in elderly subjects are feasible, which would allow the potential of NMN in improving cerebromicrovascular and cognitive outcomes to be evaluated.

Declaration of interest

D.A.S. was supported by the Glenn Foundation for Medical Research and grants from the NIH (R37 AG028730, R01 AG019719, R21 DE027490 and R01 DK100263).

D.A.S. is a founder, equity owner, board member, advisor to, director of, consultant to, investor in and/or inventor on patents licensed to Vium, Jupiter Orphan Therapeutics, Cohbar, Galilei Biosciences, GlaxoSmithKline, OvaScience, EMD Millipore, Wellomics, Inside Tracker, Caudalie, Bayer Crop Science, Longwood Fund, Zymo Research, EdenRoc Sciences (and affiliates Arc-Bio, Dovetail Genomics, Claret Bioscience, Revere Biosensors, UpRNA and MetroBiotech (an NAD booster company), Liberty Biosecurity), Life Biosciences (and affiliates Selphagy, Senolytic Therapeutics, Spotlight Biosciences, Animal Biosciences, Iduna, Immetas, Prana, Continuum Biosciences, Jumpstart Fertility (an NAD booster company), and Lua Communications). D.A.S. sits on the board of directors of both companies. D.A.S. is an inventor on a patent application filed by Mayo Clinic and Harvard Medical School that has been licensed to Elysium Health; his personal royalty share is directed to the Sinclair lab. For more information see https://genetics.med.harvard.edu/sinclair-test/people/sinclair-other.php.

Author contribution

The experiments were conducted in the Reynolds Oklahoma Center

on Aging, University of Oklahoma, Oklahoma City, OK USA. ST, PT, MNVA, AY, AC, and ZU designed the experiments; PT, ST, AC, MNVA, AY, ZT, GAF, TK, PH, TG, MK, PB, FD, ZS and EF performed and analyzed the experiments; ST, PT, MNVA, JAB, DS, AC, and ZU interpreted the data, ST, AC and ZU wrote the manuscript and DS, JAB, EF, PB, TK and MNVA revised the manuscript. All authors approved the final version of the manuscript.

Acknowledgement

This work was supported by grants from the American Heart Association (ST, MNVA, ZT, ZU and AC), the Oklahoma Center for the Advancement of Science and Technology (to AC, AY, ZU), the National Institute on Aging (R01-AG047879; R01-AG038747; R01-AG055395; R01-AG043483), the National Institute of Neurological Disorders and Stroke (NINDS; R01-NS056218 to AC, R01-NS100782 to ZU), the National Heart, Lung, and Blood Institute (R01-HL132553), the National Institute of Diabetes and Digestive and Kidney Diseases (R01-DK098656)the NIA-supported Oklahoma Nathan Shock Center (to ZU and AC; 3P30AG050911-02S1), the Oklahoma Shared Clinical and Translational Resources (OSCTR) program funded by the National Institute of General Medical Sciences (GM104938, to AY), the Presbyterian Health Foundation (to ZU, AC, AY, FD). We thank Rheal A. Towner, Ph.D., the Director of the Advanced Magnetic Resonance Center at Oklahoma Medical Research Foundation for assistance with the performance of the small-animal MRI scans that greatly improved the manuscript. The authors acknowledge the support from the NIA-funded Geroscience Training Program in Oklahoma (T32AG052363). The funding sources had no role in the study design; in the collection, analysis and interpretation of data; in the writing of the report; and in the decision to submit the article for publication.

Appendix A. Supplementary data

Supplementary data to this article can be found online at https://doi.org/10.1016/j.redox.2019.101192.

References

[1] S. Tarantini, C.H. Tran, G.R. Gordon, Z. Ungvari, A. Csiszar, Impaired neurovascular coupling in aging and Alzheimer's disease: contribution of astrocyte dysfunction and endothelial impairment to cognitive decline, Exp. Gerontol. 94 (2016), https://doi.org/10.1016/j.exger.2016.11.004.

[2] P. Toth, S. Tarantini, A. Csiszar, Z. Ungvari, Functional vascular contributions to cognitive impairment and dementia: mechanisms and consequences of cerebral autoregulatory dysfunction, endothelial impairment, and neurovascular uncoupling in aging, Am. J. Physiol. Heart Circ. Physiol. 312 (2017) H1–H20.

[3] P. Toth, S. Tarantini, A. Davila, M.N. Valcarcel-Ares, Z. Tucsek, B. Varamini, P. Ballabh, W.E. Sonntag, J.A. Baur, A. Csiszar, Z. Ungvari, Purinergic glio-endothelial coupling during neuronal activity: role of P2Y1 receptors and eNOS in functional hyperemia in the mouse somatosensory cortex, Am. J. Physiol. Heart Circ. Physiol. 309 (2015) H1837–H1845.

[4] P. Toth, S. Tarantini, Z. Tucsek, N.M. Ashpole, D. Sosnowska, T. Gautam, P. Ballabh, A. Koller, W.E. Sonntag, A. Csiszar, Z.I. Ungvari, Resveratrol treatment rescues neurovascular coupling in aged mice:role of improved cerebromicrovascular endothelial function and down-regulation of NADPH oxidas, Am. J. Physiol. Heart Circ. Physiol. 306 (2014) H299–H308.

[5] M. Zaletel, M. Strucl, J. Pretnar-Oblak, B. Zvan, Age-related changes in the relationship between visual evoked potentials and visually evoked cerebral blood flow velocity response, Funct. Neurol. 20 (2005) 115–120.

[6] M.A. Topcuoglu, H. Aydin, E. Saka, Occipital cortex activation studied with simultaneous recordings of functional transcranial Doppler ultrasound (fTCD) and visual evoked potential (VEP) in cognitively normal human subjects: effect of healthy aging, Neurosci. Lett. 452 (2009) 17–22.

[7] I. Stefanova, T. Stephan, S. Becker-Bense, T. Dera, T. Brandt, M. Dieterich, Age-related changes of blood-oxygen-level-dependent signal dynamics during optokinetic stimulation, Neurobiol. Aging 34 (2013) 2277–2286.

[8] M. Fabiani, B.A. Gordon, E.L. Maclin, M.A. Pearson, C.R. Brumback-Peltz, K.A. Low, E. McAuley, B.P. Sutton, A.F. Kramer, G. Gratton, Neurovascular coupling in normal aging: a combined optical, ERP and fMRI study, Neuroimage 85 (Pt 1) (2014 Jan 15) 592–607, https://doi.org/10.1016/j.neuroimage.2013.04.113 Epub 2013 May 9.

[9] L. Park, J. Anrather, H. Girouard, P. Zhou, C. Iadecola, Nox2-derived reactive oxygen species mediate neurovascular dysregulation in the aging mouse brain, J. Cereb. Blood Flow Metab. 27 (2007) 1908–1918.

[10] F.A. Sorond, S. Hurwitz, D.H. Salat, D.N. Greve, N.D. Fisher, Neurovascular coupling, cerebral white matter integrity, and response to cocoa in older people, Neurology 81 (10) (Sep 3 2013) 904–909, https://doi.org/10.1212/WNL.0b013e3182a351aa Epub 2013 Aug 7.

[11] F.A. Sorond, D.K. Kiely, A. Galica, N. Moscufo, J.M. Serrador, I. Iloputaife, S. Egorova, E. Dell'Oglio, D.S. Meier, E. Newton, W.P. Milberg, C.R. Guttmann, L.A. Lipsitz, Neurovascular coupling is impaired in slow walkers: the MOBILIZE boston study, Ann. Neurol. 70 (2011) 213–220.

[12] S. Tarantini, P. Hertelendy, Z. Tucsek, M.N. Valcarcel-Ares, N. Smith, A. Menyhart, E. Farkas, E. Hodges, R. Towner, F. Deak, W.E. Sonntag, A. Csiszar, Z. Ungvari, P. Toth, Pharmacologically-induced neurovascular uncoupling is associated with cognitive impairment in mice, J. Cereb. Blood Flow Metab. 35 (2015) 1871–1881.

[13] S. Tarantini, N.M. Valcarcel-Ares, A. Yabluchanskiy, G.A. Fulop, P. Hertelendy, T. Gautam, E. Farkas, A. Perz, P.S. Rabinovitch, W.E. Sonntag, A. Csiszar, Z. Ungvari, Treatment with the mitochondrial-targeted antioxidant peptide SS-31 rescues neurovascular coupling responses and cerebrovascular endothelial function and improves cognition in aged mice, Aging Cell 17 (2018).

[14] C.A. Oomen, E. Farkas, V. Roman, E.M. van der Beek, P.G. Luiten, P. Meerlo, Resveratrol preserves cerebrovascular density and cognitive function in aging mice, Front. Aging Neurosci. 1 (2009) 4.

[15] A. Das, G.X. Huang, M.S. Bonkowski, A. Longchamp, C. Li, M.B. Schultz, L.J. Kim, B. Osborne, S. Joshi, Y. Lu, J.H. Trevino-Villarreal, M.J. Kang, T.T. Hung, B. Lee, E.O. Williams, M. Igarashi, J.R. Mitchell, L.E. Wu, N. Turner, Z. Arany, L. Guarente, D.A. Sinclair, Impairment of an endothelial NAD(+)-H2S signaling network is a reversible cause of vascular aging, Cell 173 (2018) 74–89 e20.

[16] A. Csiszar, N. Labinskyy, R. Jimenez, J.T. Pinto, P. Ballabh, G. Losonczy, K.J. Pearson, R. de Cabo, Z. Ungvari, Anti-oxidative and anti-inflammatory vasoprotective effects of caloric restriction in aging: role of circulating factors and SIRT1, Mech. Ageing Dev. 130 (2009) 518–527.

[17] A. Csiszar, N. Labinskyy, J.T. Pinto, P. Ballabh, H. Zhang, G. Losonczy, K.J. Pearson, R. de Cabo, P. Pacher, C. Zhang, Z.I. Ungvari, Resveratrol induces mitochondrial biogenesis in endothelial cells, Am. J. Physiol. Heart Circ. Physiol. 297 (1) (2009 Jul) H13–H20, https://doi.org/10.1152/ajpheart.00368.2009 Epub 2009 May 8.

[18] A. Csiszar, N. Labinskyy, A. Podlutsky, P.M. Kaminski, M.S. Wolin, C. Zhang, P. Mukhopadhyay, P. Pacher, F. Hu, R. de Cabo, P. Ballabh, Z. Ungvari, Vasoprotective effects of resveratrol and SIRT1: attenuation of cigarette smoke-induced oxidative stress and proinflammatory phenotypic alterations, Am. J. Physiol. Heart Circ. Physiol. 294 (2008) H2721–H2735.

[19] A.P. Gomes, N.L. Price, A.J. Ling, J.J. Moslehi, M.K. Montgomery, L. Rajman, J.P. White, J.S. Teodoro, C.D. Wrann, B.P. Hubbard, E.M. Mercken, C.M. Palmeira, R. de Cabo, A.P. Rolo, N. Turner, E.L. Bell, D.A. Sinclair, Declining NAD(+) induces a pseudohypoxic state disrupting nuclear-mitochondrial communication during aging, Cell 155 (2013) 1624–1638.

[20] H. Massudi, R. Grant, N. Braidy, J. Guest, B. Farnsworth, G.J. Guillemin, Age-associated changes in oxidative stress and NAD+ metabolism in human tissue, PLoS One 7 (2012) e42357.

[21] R.M. Anderson, K.J. Bitterman, J.G. Wood, O. Medvedik, H. Cohen, S.S. Lin, J.K. Manchester, J.I. Gordon, D.A. Sinclair, Manipulation of a nuclear NAD+ salvage pathway delays aging without altering steady-state NAD+ levels, J. Biol. Chem. 277 (2002) 18881–18890.

[22] S.J. Mitchell, M. Bernier, M.A. Aon, S. Cortassa, E.Y. Kim, E.F. Fang, H.H. Palacios, A. Ali, I. Navas-Enamorado, A. Di Francesco, T.A. Kaiser, T.B. Waltz, N. Zhang, J.L. Ellis, P.J. Elliott, D.W. Frederick, V.A. Bohr, M.S. Schmidt, C. Brenner, D.A. Sinclair, A.A. Sauve, J.A. Baur, R. de Cabo, Nicotinamide improves aspects of healthspan, but not lifespan, in mice, Cell Metabol. 27 (2018) 667–676 e4.

[23] J. Yoshino, J.A. Baur, S.I. Imai, NAD(+) intermediates: the biology and therapeutic potential of NMN and NR, Cell Metabol. 27 (2018) 513–528.

[24] K.F. Mills, S. Yoshida, L.R. Stein, A. Grozio, S. Kubota, Y. Sasaki, P. Redpath, M.E. Migaud, R.S. Apte, K. Uchida, J. Yoshino, S.I. Imai, Long-term administration of nicotinamide mononucleotide mitigates age-associated physiological decline in mice, Cell Metabol. 24 (2016) 795–806.

[25] N.E. de Picciotto, L.B. Gano, L.C. Johnson, C.R. Martens, A.L. Sindler, K.F. Mills, S. Imai, D.R. Seals, Nicotinamide mononucleotide supplementation reverses vascular dysfunction and oxidative stress with aging in mice, Aging Cell 15 (2016) 522–530.

[26] D.F. Dai, P.S. Rabinovitch, Z. Ungvari, Mitochondria and cardiovascular aging, Circ. Res. 110 (2012) 1109–1124.

[27] Z. Springo, S. Tarantini, P. Toth, Z. Tucsek, A. Koller, W.E. Sonntag, A. Csiszar, Z. Ungvari, Aging exacerbates pressure-induced mitochondrial oxidative stress in mouse cerebral arteries, J. Gerontol. A Biol. Sci. Med. Sci. 70 (2015) 1355–1359.

[28] Z. Ungvari, Z. Orosz, N. Labinskyy, A. Rivera, Z. Xiangmin, K. Smith, A. Csiszar, Increased mitochondrial H2O2 production promotes endothelial NF-kappaB activation in aged rat arteries, Am. J. Physiol. Heart Circ. Physiol. 293 (2007) H37–H47.

[29] Z. Ungvari, S. Tarantini, P. Hertelendy, M.N. Valcarcel-Ares, G.A. Fulop, S. Logan, T. Kiss, E. Farkas, A. Csiszar, A. Yabluchanskiy, Cerebromicrovascular dysfunction predicts cognitive decline and gait abnormalities in a mouse model of whole brain irradiation-induced accelerated brain senescence, Geroscience 39 (2017) 33–42.

[30] P. Toth, Z. Tucsek, D. Sosnowska, T. Gautam, M. Mitschelen, S. Tarantini, F. Deak, A. Koller, W.E. Sonntag, A. Csiszar, Z. Ungvari, Age-related autoregulatory dysfunction and cerebromicrovascular injury in mice with angiotensin II-induced hypertension, J. Cereb. Blood Flow Metab. 33 (2013) 1732–1742.

[31] A. Csiszar, Z. Tucsek, P. Toth, D. Sosnowska, T. Gautam, A. Koller, F. Deak, W.E. Sonntag, Z. Ungvari, Synergistic effects of hypertension and aging on cognitive function and hippocampal expression of genes involved in beta-amyloid generation

and Alzheimer's disease, Am. J. Physiol. Heart Circ. Physiol. 305 (2013) H1120–H1130.
[32] D.A. MacLaren, J.A. Santini, A.L. Russell, T. Markovic, S.D. Clark, Deficits in motor performance after pedunculopontine lesions in rats - impairment depends on demands of task, Eur. J. Neurosci. 40 (8) (2014 Oct) 3224–3236, https://doi.org/10.1111/ejn.12666 Epub 2014 Jul 4.
[33] S. Tarantini, A. Yabluchanksiy, G.A. Fulop, P. Hertelendy, M.N. Valcarcel-Ares, T. Kiss, J.M. Bagwell, D. O'Connor, E. Farkas, F. Sorond, A. Csiszar, Z. Ungvari, Pharmacologically induced impairment of neurovascular coupling responses alters gait coordination in mice, Geroscience 39 (2017) 601–614.
[34] P. Toth, S. Tarantini, Z. Springo, Z. Tucsek, T. Gautam, C.B. Giles, J.D. Wren, A. Koller, W.E. Sonntag, A. Csiszar, Z. Ungvari, Aging exacerbates hypertension-induced cerebral microhemorrhages in mice: role of resveratrol treatment in vasoprotection, Aging Cell 14 (2015) 400–408.
[35] P. Toth, S. Tarantini, N.M. Ashpole, Z. Tucsek, G.L. Milne, N.M. Valcarcel-Ares, A. Menyhart, E. Farkas, W.E. Sonntag, A. Csiszar, Z. Ungvari, IGF-1 deficiency impairs neurovascular coupling in mice: implications for cerebromicrovascular aging, Aging Cell 14 (2015) 1034–1044.
[36] K. Kazama, J. Anrather, P. Zhou, H. Girouard, K. Frys, T.A. Milner, C. Iadecola, Angiotensin II impairs neurovascular coupling in neocortex through NADPH oxidase-derived radicals, Circ. Res. 95 (2004) 1019–1026.
[37] A. Csiszar, Z. Ungvari, J.G. Edwards, P.M. Kaminski, M.S. Wolin, A. Koller, G. Kaley, Aging-induced phenotypic changes and oxidative stress impair coronary arteriolar function, Circ. Res. 90 (2002) 1159–1166.
[38] P. Pacher, J.S. Beckman, L. Liaudet, Nitric oxide and peroxynitrite in health and disease, Physiol. Rev. 87 (2007) 315–424.
[39] K.J. Pearson, J.A. Baur, K.N. Lewis, L. Peshkin, N.L. Price, N. Labinskyy, W.R. Swindell, D. Kamara, R.K. Minor, E. Perez, H.A. Jamieson, Y. Zhang, S.R. Dunn, K. Sharma, N. Pleshko, L.A. Woollett, A. Csiszar, Y. Ikeno, D. Le Couteur, P.J. Elliott, K.G. Becker, P. Navas, D.K. Ingram, N.S. Wolf, Z. Ungvari, D.A. Sinclair, R. de Cabo, Resveratrol delays age-related deterioration and mimics transcriptional aspects of dietary restriction without extending life span, Cell Metabol. 8 (2008) 157–168.
[40] Z. Ungvari, A. Csiszar, A. Huang, P.M. Kaminski, M.S. Wolin, A. Koller, High pressure induces superoxide production in isolated arteries via protein kinase C-dependent activation of NAD(P)H oxidase, Circulation 108 (2003) 1253–1258.
[41] N. Labinskyy, P. Mukhopadhyay, J. Toth, G. Szalai, M. Veres, G. Losonczy, J.T. Pinto, P. Pacher, P. Ballabh, A. Podlutsky, S.N. Austad, A. Csiszar, Z. Ungvari, Longevity is associated with increased vascular resistance to high glucose-induced oxidative stress and inflammatory gene expression in Peromyscus leucopus, Am. J. Physiol. Heart Circ. Physiol. 296 (2009) H946–H956.
[42] A. Csiszar, N. Labinskyy, Z. Orosz, Z. Xiangmin, R. Buffenstein, Z. Ungvari, Vascular aging in the longest-living rodent, the naked mole rat, Am. J. Physiol. 293 (2007) H919–H927.
[43] Z. Ungvari, A. Podlutsky, D. Sosnowska, Z. Tucsek, P. Toth, F. Deak, T. Gautam, A. Csiszar, W.E. Sonntag, Ionizing radiation promotes the acquisition of a senescence-associated secretory phenotype and impairs angiogenic capacity in cerebromicrovascular endothelial cells: role of increased DNA damage and decreased DNA repair capacity in microvascular radiosensitivity, J. Gerontol. A Biol. Sci. Med. Sci. 68 (2013) 1443–1457.
[44] K.M. Robinson, M.S. Janes, J.S. Beckman, The selective detection of mitochondrial superoxide by live cell imaging, Nat. Protoc. 3 (2008) 941–947.
[45] Z. Ungvari, N. Labinskyy, P. Mukhopadhyay, J.T. Pinto, Z. Bagi, P. Ballabh, C. Zhang, P. Pacher, A. Csiszar, Resveratrol attenuates mitochondrial oxidative stress in coronary arterial endothelial cells, Am. J. Physiol. Heart Circ. Physiol. 297 (2009) H1876–H1881.
[46] A. Csiszar, A. Podlutsky, N. Podlutskaya, W.E. Sonntag, S.Z. Merlin, E.E.R. Philipp, K. Doyle, A. Davila, F.A. Recchia, P. Ballabh, J.T. Pinto, Z. Ungvari, Testing the oxidative stress hypothesis of aging in primate fibroblasts: is there a correlation between species longevity and cellular ROS production? J. Gerontol. A Biol. Sci. Med. Sci. 67 (2012) 841–852.
[47] A. Csiszar, D. Sosnowska, M. Wang, E.G. Lakatta, W.E. Sonntag, Z. Ungvari, Age-associated proinflammatory secretory phenotype in vascular smooth muscle cells from the non-human primate Macaca mulatta: reversal by resveratrol treatment, J. Gerontol. A Biol. Sci. Med. Sci. 67 (2012) 811–820.
[48] P. Mukhopadhyay, M. Rajesh, G. Hasko, B.J. Hawkins, M. Madesh, P. Pacher, Simultaneous detection of apoptosis and mitochondrial superoxide production in live cells by flow cytometry and confocal microscopy, Nat. Protoc. 2 (2007) 2295–2301.
[49] M.J. Karnowsky, A formaldehyde-glutaraldehyde fixative of high osmolarity for use in electron microscopy, J. Cell Biol. 27 (1965) 137–138.
[50] Z.I. Ungvari, N. Labinskyy, S.A. Gupte, P.N. Chander, J.G. Edwards, A. Csiszar, Dysregulation of mitochondrial biogenesis in vascular endothelial and smooth muscle cells of aged rats, Am. J. Physiol. Heart Circ. Physiol. 294 (2008) H2121–H2128.
[51] E.R. Weibel, Stereological principles for morphometry in electron microscopic cytology, Int. Rev. Cytol. 26 (1969) 235–302.
[52] Z. Tucsek, M. Noa Valcarcel-Ares, S. Tarantini, A. Yabluchanskiy, G. Fulop, T. Gautam, A. Orock, A. Csiszar, F. Deak, Z. Ungvari, Hypertension-induced synapse loss and impairment in synaptic plasticity in the mouse hippocampus mimics the aging phenotype: implications for the pathogenesis of vascular cognitive impairment, Geroscience 39 (4) (2017 Aug) 385–406, https://doi.org/10.1007/s11357-017-9981-y Epub 2017 Jun 29.
[53] Z. Ungvari, G. Kaley, R. de Cabo, W.E. Sonntag, A. Csiszar, Mechanisms of vascular aging: new perspectives, J. Gerontol. A Biol. Sci. Med. Sci. 65 (2010) 1028–1041.
[54] C.S. Kinter, J.M. Lundie, H. Patel, P.M. Rindler, L.I. Szweda, M. Kinter, A quantitative proteomic profile of the Nrf2-mediated antioxidant response of macrophages to oxidized LDL determined by multiplexed selected reaction monitoring, PLoS One 7 (2012) e50016.
[55] P. Pacher, J.G. Mabley, F.G. Soriano, L. Liaudet, K. Komjati, C. Szabo, Endothelial dysfunction in aging animals: the role of poly(ADP-ribose) polymerase activation, Br. J. Pharmacol. 135 (2002) 1347–1350.
[56] R.A. Gioscia-Ryan, T.J. LaRocca, A.L. Sindler, M.C. Zigler, M.P. Murphy, D.R. Seals, Mitochondria-targeted antioxidant (MitoQ) ameliorates age-related arterial endothelial dysfunction in mice, J. Physiol. 592 (2014) 2549–2561.
[57] L.K. Kwong, R.S. Sohal, Age-related changes in activities of mitochondrial electron transport complexes in various tissues of the mouse, Arch. Biochem. Biophys. 373 (2000) 16–22.
[58] A. Csiszar, S. Tarantini, A. Yabluchanskiy, P. Balasubramanian, T. Kiss, E. Farkas, J.A. Baur, Z.I. Ungvari, Role of endothelial NAD+ deficiency in age-related vascular dysfunction, Am. J. Physiol. Heart Circ. Physiol. (2019 Mar 15), https://doi.org/10.1152/ajpheart.00039.2019 Epub ahead of print.
[59] D.B. Zorov, M. Juhaszova, S.J. Sollott, Mitochondrial reactive oxygen species (ROS) and ROS-induced ROS release, Physiol. Rev. 94 (2014) 909–950.
[60] B. Gong, Y. Pan, P. Vempati, W. Zhao, L. Knable, L. Ho, J. Wang, M. Sastre, K. Ono, A.A. Sauve, G.M. Pasinetti, Nicotinamide riboside restores cognition through an upregulation of proliferator-activated receptor-gamma coactivator 1alpha regulated beta-secretase 1 degradation and mitochondrial gene expression in Alzheimer's mouse models, Neurobiol. Aging 34 (2013) 1581–1588.
[61] E.F. Fang, H. Kassahun, D.L. Croteau, M. Scheibye-Knudsen, K. Marosi, H. Lu, R.A. Shamanna, S. Kalyanasundaram, R.C. Bollineni, M.A. Wilson, W.B. Iser, B.N. Wollman, M. Morevati, J. Li, J.S. Kerr, Q. Lu, T.B. Waltz, J. Tian, D.A. Sinclair, M.P. Mattson, H. Nilsen, V.A. Bohr, NAD(+) replenishment improves lifespan and healthspan in ataxia telangiectasia models via mitophagy and DNA repair, Cell Metabol. 24 (2016) 566–581.
[62] A.N. Long, K. Owens, A.E. Schlappal, T. Kristian, P.S. Fishman, R.A. Schuh, Effect of nicotinamide mononucleotide on brain mitochondrial respiratory deficits in an Alzheimer's disease-relevant murine model, BMC Neurol. 15 (2015) 19.
[63] J. Yoshino, K.F. Mills, M.J. Yoon, S. Imai, Nicotinamide mononucleotide, a key NAD(+) intermediate, treats the pathophysiology of diet- and age-induced diabetes in mice, Cell Metabol. 14 (2011) 528–536.
[64] Z. Tucsek, P. Toth, S. Tarantini, D. Sosnowska, T. Gautam, J.P. Warrington, C.B. Giles, J.D. Wren, A. Koller, P. Ballabh, W.E. Sonntag, Z. Ungvari, A. Csiszar, Aging exacerbates obesity-induced cerebromicrovascular rarefaction, neurovascular uncoupling, and cognitive decline in mice, J. Gerontol. A Biol. Sci. Med. Sci. 69 (2014) 1339–1352.
[65] H.J. Lee, D. Feliers, J.L. Barnes, S. Oh, G.G. Choudhury, V. Diaz, V. Galvan, R. Strong, J. Nelson, A. Salmon, C.G. Kevil, B.S. Kasinath, Hydrogen sulfide ameliorates aging-associated changes in the kidney, Geroscience 40 (2018) 163–176.
[66] N.L. Kanagy, C.G. Kevil, The pleiotropic effects of hydrogen sulfide, Am. J. Physiol. Heart Circ. Physiol. 314 (2018) H1–H2.
[67] Clinical Trial registration number UMIN000021309: assessment of the safety of nicotinamide mononucleotide (NMN) in healthy subjects; phase I study. The clinical trial to evaluate metabolic-syndrome-related parameters to develop NMN as Foods with Function Claims, Available at: https://upload.umin.ac.jp/cgi-open-bin/ctr/ctr.cgi?function=brows&action=brows&type=summary&language=J&recptno=R000024575 , Accessed date: 23 September 2017.